

*A Major-2 project report  
On*

***A STUDY ON EFFECT OF JOINT ORIENTATION ON STRENGTH AND  
DEFORMATION BEHAVIOUR OF JOINTED ROCK***

*Submitted in the partial fulfillment of the requirements for the award of the  
degree of*

***MASTER OF TECHNOLOGY***

*In*

***GEOTECHNICAL ENGINEERING***

*Submitted by*

**(AVANISH KUMAR)**

**(2K15/GTE/06)**

**(Fourth Semester)**

*Under the Guidance of*

**Dr. A. K. Shrivastava**

**(Associate Professor)**



**Department of Civil Engineering,**

**Delhi Technological University**

***(Formerly Delhi college of Engineering, DCE)***

**Govt. of NCT of Delhi**

**Main Bawana Road, Delhi-110042**

## **CANDIDATE'S DECLARATION**

I do hereby certify that the work presented is the report entitled “**A study on effect of joint orientation on strength and deformation behaviour of jointed rock**” in the partial fulfilment of the requirements for the award of the degree of “Master Of Technology in Geotechnical Engineering” submitted in the department of Civil Engineering, Delhi Technological University, is an authentic record of our own work carried from January’1 to july’ 20 under the supervision of Dr.A.K. Shrivastava, Department of Civil Engineering.

I have not submitted the matter embodied in the report for the award of any other degree or diploma.

Date :20-july-2017

Avanish Kumar  
(2K15/GTE/06)

---

## **CERTIFICATE**

This is to certify that the above statement made by the candidate is correct to best of my knowledge.

Dr. A.K.Shrivastava  
Associate Professor  
Department of Civil Engineering  
Delhi Technological University

## **ACKNOWLEDGEMENT**

I take this opportunity to express my gratitude and deep regards to Dr. Amit Kumar Shrivastava (Associate Professor, Civil Engineering Department, DTU ) for his guidance, monitoring and constant encouragement throughout the course of this project work. The blessing, help and guidance given by him from time to time shall carry me a long way in life on which I am going to embark.

I would also like to thank Dr. Nirendra Dev (Head of Department, Civil Engineering Department, DTU) for extending his support and guidance.

Professors and faculties of the Department of Civil Engineering, DTU, have always extended their full co-operation and help. They have been kind enough to give their opinions on the project matter; I am deeply obliged to them. They have been a source of encouragement and have continuously been supporting me with their knowledge base, during the study.

Avanish Kumar  
M. Tech (Geotechnical Engineering)  
Roll No. 2K15/GTE/06  
Department of Civil Engineering  
Delhi Technological University, Delhi

## INDEX

<b>Contents</b>	<b>Page No.</b>
Abstract	vi
List of figures	vii - viii
List of tables	ix - x
Notations	xi
Chapter 1: Introduction	1-4
1.1 Objective of work	3
1.2 Organization of thesis	3-4
Chapter 2: Literature review	5-8
Chapter 3: Laboratory investigation	9-19
3.1 Experimental programme	9-17
3.1.1 Direct shear test	10
3.1.2 Uniaxial compressive strength test	10-17
3.2 Materials used	18
3.3 Model of Specimen	18
3.4 Preparation of Specimens	19
3.5 Curing	19
3.6 Making joints in specimens	19
Chapter 4: Results and discussions	20-39
4.1 Direct shear test results	20-21
4.2 Uniaxial compression test results	21-28
4.3 Parameter studied	28
4.4 Comparison of results with empirical formulae	29- 39
Chapter 5: Development of prediction model	40-49
Conclusions	50
Scope of future work	51



## **Abstract**

Rock is different from other type of engineering material available. That is why designing and building structure in rock is a difficult practice. A detailed literature review on unlike aspects of jointed rock mass show that the jointed rock mass behaviours effected by numerous factors such as joints locations, joint frequency, and orientation of joints and strengths of joints. In the present tudy, an approach has been made to setup empirical relation to express the jointed rock properties as a function of properties of intact rock and joint factor ( $J_f$ ). Joint factor is an important parameter in jointed rock mass and the influence of joints in the jointed rock mass is taken into account by the joint factor in the jointed rock mass. There are following supreme significant factors, which are responsible for the strength of rock mass are presence of cracks in rock, presence of fault, fissures, rocks type, bedding planes, Joint surface type, and minerals presence in the bedding planes etc. All these factors also play a significant role in the strength and deformation behaviour of jointed rock mass. As in-situ computation of jointed rock mass is very time consuming and very expensive. An effort has been made to predict the strength and deformation of rock mass through the test conducted on model material test in laboratory conditions.

In rock Engineering and design of rock structure, rock mass classification systems have been popular and are rapidly used. All of these Rock classification systems have their own limitations, but can be used as approximation with the care, as they are very useful tools. Different type of joint arrangements has been introduced to see the most common types of failure occur in jointed rock mass. Plaster of paris and plaster of paris-sand mix has been used as model material. The specimen have been prepared by using model materials, plaster of paris and sand-plaster of Paris mix. In specimen, different degrees of anisotropy have been introduced by creating joints in specimen from zero degree to ninety degree ( $0^\circ$  to  $90^\circ$ ). There are two type of test performed on the specimen: (i) Direct shear test, (ii) Uniaxial compression test, has been performed in order to classify the single jointed and double jointed rock mass, artificially made of plaster of paris and plaster of paris-sand mix. These tests have been performed to find out the numerous parameters such as modulus ratio, strength ratio, uniaxial compressive strength etc. This classification can thereafter give a probable direction of Rock engineering design concept.

• LIST OF FIGURES

Figure No.	Title	Page No.
Figure 1.1	Splitting and shearing mode of failure	7
Figure 1.2	Rotation and sliding modes of failure	8
Figure 3.1	Flow chat of experimental programme	9
Figure 3.1.1	Direct shear test	10
Figure 3.1.2	Uniaxial compressive test for intact rock specimen	12
Figure 3.1.3	Uniaxial compressive test for jointed rock specimen	13
Figure 3.1.4	Failure of intact specimen	14
Figure 3.1.5	Types of joints studied (single jointed) in plaster of paris specimens and sand- plaster of paris mix specimens	15
Figure 3.1.6	Types of joints studied (double jointed) in plaster of paris specimens and sand- plaster of paris mix specimens	27
Figure 3.3.1	Dimension of specimen	18
Figure 4.1.1	Graph between normal stress and shear stress( plaster of paris)	20
Figure 4.1.2	Graph between normal stress and shear stress(plaster of paris- sand mix)	21
Figure 4.2.1	Graph between water content and uniaxial compressive strength (plaster of paris)	22
Figure 4.2.2	Graph between water content and uniaxial compressive strength (plaster of paris-sand mix)	23
Figure 4.2.3	stress-strain curve (plaster of paris)	24
Figure 4.2.4	stress-strain curve (Plaster of paris- sand mixture)	26
Figure 4.2.5	Graph between joint orientation angle $\beta$ and uniaxial compressive strength (MPa) (plaster of paris)	27
Figure 4.2.6	Graph between joint orientation angle $\beta$ and uniaxial compressive strength (MPa) (plaster of paris - sand )	28
Figure 4.4.1	Graph between joint factor, $J_f$ and strength ratio $\sigma_{cr}$ (single jointed)	30
Figure 4.4.2	Graph between joint factor, $J_f$ and modulus ratio $E_r$ (single jointed)	31
Figure 4.4.3	Graph between joint factor, $J_f$ and strength ratio $\sigma_{cr}$ (double jointed)	32
Figure 4.4.4	Graph between joint factor, $J_f$ and modulus ratio $E_r$ (double jointed)	33
Figure 4.4.5	Comparison of single jointed and double jointed orientation angle $\beta$ of plaster of paris	34
Figure 4.4.6	Graph between joint factor $J_f$ and strength ratio $\sigma_r$ (single jointed)	35
Figure 4.4.7	Graph between joint factor $J_f$ and elastic modulus $E_r$ (single jointed)	36
Figure 4.4.8	Graph between joint factor $J_f$ and strength ratio $\sigma_r$ (double jointed)	37
Figure 4.4.9	Graph between joint factor $J_f$ and modulus ratio $E_r$ ( double jointed)	38
Figure 4.4.10	Comparison of orientation angle $\beta$ of single and double Jointed specimen of plaster of paris- sand mix	39

Figure 5.1	Comparison of uniaxial compressive strength ratio of prediction model with present study and empirical formulae (jointed specimen of plaster of paris, single joint)	42
Figure 5.2	Comparison of elastic modulus ratio of prediction model with present study and empirical formulae (jointed specimen of plaster of paris, Single joint)	43
Figure 5.3	Comparison of uniaxial compressive strength ratio of prediction model with present study and empirical formulae (jointed specimen of plaster of paris, double joint)	44
Figure 5.4	Comparison of elastic modulus ratio of prediction model with present study and empirical formulae (jointed specimen of plaster of paris, double joint)	45
Figure 5.5	Comparison of uniaxial compressive strength ratio of prediction model with present study and empirical formulae (jointed specimen of plaster of paris-sand mix, single joint)	46
Figure 5.6	Comparison of elastic modulus ratio of prediction model with present study and empirical formulae (jointed specimen of plaster of paris-sand mix, single joint)	47
Figure 5.7	Comparison of uniaxial compressive strength ratio of prediction model with present study and empirical formulae (jointed specimen of plaster of paris-sand mix, double joint)	48
Figure 5.8	Comparison of elastic modulus ratio of prediction model with present study and empirical formulae ( jointed specimen of plaster of paris, double joint):	49



• LIST OF TABLES

Table No.	Title No.	Page No.
Table : 1.1	The value of inclination parameter, n (Ramamurty ,1993)	02
Table : 1.2	Strength of jointed and intact rock mass	03
Table : 1.3	Modulus ratio classification of intact and jointed rocks	03
Table : 3.1.1	Uniaxial compression test (single joint)	14
Table : 3.1.2	Uniaxial compression test ( double joints)	16
Table : 4.1.1	Values of shear stress for different values of normal stress on specimens of plaster of paris in direct shear stress test	20
Table : 4.1.1	Values of shear stress for different values of normal stress on specimens of plaster of paris-sand mixture in direct shear stress test	21
Table : 4.2.1	Uniaxial compressive strength (MPa) values against water content (%) for plaster of paris	21
Table : 4.2.2	Uniaxial compressive strength (MPa) values against water content (%) for plaster of paris- sand mix	22
Table : 4.2.3	Values of stress and strain for intact specimens of plaster of paris	23-24
Table : 4.2.4	Values of stress and strain for intact specimens of plaster of paris-sand mix	25
Table : 4.2.5	Uniaxial compressive strength, $\sigma_{cj}$ (MPa) values corresponding to orientation angle ( $\beta^\circ$ ) of plaster of paris jointed specimen	26
Table : 4.2.6	Uniaxial compressive strength, $\sigma_{cj}$ (MPa) values corresponding to orientation angle ( $\beta^\circ$ ) of plaster of paris- sand mixture jointed specimen	27
Table : 4.3.1	Physical and engineering properties of plaster of paris used for joints studied	28
Table : 4.3.2	Physical and engineering properties of plaster of paris-sand mixture used for joints studied	28
Table : 4.4.1	Value of $J_n$ , $J_f$ , $\sigma_{cj}$ , $\sigma_{cr}$ for jointed specimen of plaster of paris (Single joint)	30
Table : 4.4.2	Value of $E_{tj}$ , $E_r$ , $J_n$ , and $J_f$ for jointed specimens of plaster of paris (Single joint)	31
Table : 4.4.3	Value OF $J_n$ , $J_f$ , $\sigma_{cj}$ , $\sigma_{cr}$ For plaster of paris jointed specimens (double joint)	32
Table : 4.4.4	Value OF $E_{tj}$ , $E_r$ , $J_n$ and $J_f$ for plaster of paris jointed specimens (double joints)	33
Table : 4.4.5	Values of $J_n$ , $J_f$ , $\sigma_{cj}$ , $\sigma_{cr}$ for jointed specimens of sand- plaster of paris mixture (single joint)	35

Table : 4.4.6	Values OF $E_{tj}$ , $E_r$ , $J_n$ and $J_f$ for jointed specimens of sand – plaster of paris mix (single joint)	36
Table : 4.4.7	Values of $J_n$ , $J_f$ , $\sigma_{cj}$ , $\sigma_{cr}$ for jointed specimen of sand- plaster of paris mix (double joint)	37
Table : 4.4.8	Value of $E_{tj}$ , $E_r$ , $J_n$ and $J_f$ for specimen of sand-plaster of paris mix (double joints)	38
Table : 5.1	Comparison of uniaxial compressive strength ratio of Prediction model with present study and empirical formulae ( jointed specimen of plaster of paris, single joint)	41
Table : 5.2	Comparison of elastic modulus ratio of Prediction model with present study and empirical formulae ( jointed specimen of plaster of paris, Single joint)	42
Table : 5.3	Comparison of uniaxial compressive strength ratio of Prediction model with present study and empirical formulae ( jointed specimen of plaster of paris, double joint)	43
Table : 5.4	Comparison of elastic modulus ratio of Prediction model with present study and empirical formulae ( jointed specimen of plaster of paris, double joint)	44
Table : 5.5	Comparison of uniaxial compressive strength ratio of Prediction model with present study and empirical formulae ( jointed specimen of plaster of paris-sand mix, single joint)	45
Table : 5.6	Comparison of elastic modulus ratio of Prediction model with present study and empirical formulae ( jointed specimen of plaster of paris-sand mix, single joint)	46
Table : 5.7	Comparison of uniaxial compressive strength ratio of Prediction model with present study and empirical formulae ( jointed specimen of plaster of paris-sand mix, double joint)	47
Table : 5.8	Comparison of elastic modulus ratio of Prediction model with present study and empirical formulae ( jointed specimen of plaster of paris, double joint):	48



## • NOTATIONS

**$J_f$  = Joint factor**

**$J_n$  = Number of joints per metre length.**

**$n$  = Joint inclination parameter**

**$r$  = Roughness parameter.**

**$\beta$  = orientation of joint.**

**$i$  = Inclination of the asperity**

**$\sigma_j$  = Uniaxial compressive strength of jointed rock**

**$\sigma_i$  = Uniaxial compressive strength of intact rock**

**$\sigma_{cr}$  = Uniaxial compressive strength ration.**

**$E_j$  = Tangent modulus of jointed rock**

**$E_i$  = Tangent modulus of intact rock**

**$E_r$  = Elastic modulus ratio**

**$\tau$  = Shear strength**

**$\sigma_n$  = Normal stress**

**$\phi$  = angle of friction**

## **Chapter-1**

### **Introduction**

Common geographical conditions are normally very complicated. In India, the geology is diverse and complex. Rock held as a different field of engineering and effective from engineering geography. It is not manages only with rock mass as building materials as well as manages changes in mechanical behaviour in rocks, for example, stress, strain and movements in rocks brought in due to designing activities. It is also associated with design and stability of underground structures in rocks. Rocks are not as closely homogeneous and isotropic as, many other engineering materials . Rocks are discontinuous medium with the faults, fractures, joints, folds, fissures, bedding planes, shear zones and many other structural features, which may exert significant influence on their engineering responses. The discontinuities such as faults, fractures, joints, folds , fissures, bedding planes, shear zone, etc may be exist with or without gouge material. The strength of rock masses mainly depends on the behaviour of these discontinuities or planes of weaknesses. The frequency of joints present in the rock mass and their orientation with respect to the engineering structures, and the roughness of the joint have a important significance from the stability point of view. Reliable classification of the strength and deformation behaviour of jointed rocks mass is essential for safedesign of civil structures such as dams, buildings, metro and road tunnels, bridge piers, etc. Intact rock mass properties, discontinuities in jointed rock mass and the properties of the joints can be determined in the laboratory where as direct physical measurements of the properties of the rock mass are very costly as compared to laboratory study. Artificial anisotropy have been introduce and studied mainly as they have the advantage of being re-create. The anisotropic strength behaviour of slates, gypsum and shale has been studied by a large number of investigators. Laboratory studies carried by many researcher shows that many different failure modes are possible in jointed rock and that the internal distribution of stresses within a jointed rock mass can be extremely complex.

A fair assessment of strength behaviour of jointed rock mass is essential for the design of slope foundations, underground openings and anchoring systems. The problems of making predictions of the engineering responses of rock masses derive largely from their discontinuous and variable nature. The strength behaviour of rock mass is governed by couple of things such as intact rock properties and properties of discontinuities. The strength of rock and rock mass depends on numerous factors as follows:

1. The angle made by the joint with the principal stress direction.
2. The degree of joint separation.
3. Opening of the joint
4. Number of joints in a given direction
5. Strength along the joint
6. Joint roughness
7. Joint frequency

The current study aims to link relation between the ratios of intact and joint rock mass strength with joint factor  $J_f$  and also with other factors. The significant factors, which influence the modulus value and strength of jointed rock mass are as follow:

- (i) Joint frequency,  $J_n$ ,
- (ii) Joint strength.
- (iii) Joint orientation,  $\beta$ , with respect to major principal stress direction and

These effects can be incorporated into a Joint factor by Arora (1987) as,

$$J_f = J_n / (n \cdot r)$$

Where,

$J_n$  is the number of joints per meter depth,

' $r$ ' is a roughness parameter depending on the joint condition, and

' $n$ ' is an inclination parameter depending on the orientation of the joint  $\beta$ ,

The value of ' $n$ ' is found by taking the ratio of log (strength reduction) at  $\beta = 90^\circ$  to log (strength reduction) at the desired value of  $\beta$ . This inclination parameter is independent on joint frequency. The values of inclination parameter ' $n$ ' are given for various orientation angles in tabular form in table 1.1 (Ramamurthy, 1994). The joint strength parameter ' $r$ ' is obtained from the shear test along the joint.

**Table 1.1:** The value of inclination parameter,  $n$  (Ramamurthy, 1993):

Orientation of joint $\beta^\circ$	Inclination parameter $n$
0	0.810
10	0.46
20	0.105
30	0.046
40	0.071
50	0.306
60	0.465
70	0.634
80	0.814
90	1.00

Ramamurthy and Arora (1993) classify intact rock mass on the basis of uniaxial compressive strength (table 1.2) and elastic modulus (table 1.3) of intact rock mass.

**Table 1.2:** Strength of jointed and intact rock mass (Ramamurthy and Arora, 1993)

Class	Description	UCS, MPa
A	Very high strength	>250
B	High strength	100-250
C	Moderate strength	50-100
D	Medium strength	25-50
E	Low strength	5-25
F	Very low strength	<5

**Table 1.3:** Modulus ratio classification of intact and jointed rocks (Ramamurthy and Arora, 1993)

Class	Description	Modulus ratio
A	Very high modulus ratio	>500
B	High modulus ratio	200-500
C	Medium modulus ratio	100-200
D	Low modulus ratio	50-100
E	Very low modulus ratio	<50

**1.1 Objective of work:**

In order to understand the behaviour of jointed rock masses, it is necessary to have a clear understanding of strength and deformation behaviour of jointed rock mass. A fair assessment of strength behaviour of jointed rock mass is essential for the design of slope foundations, underground openings and anchoring systems. The problems of making predictions of the engineering responses of rock masses derive largely from their discontinuous and variable nature. So by noticing the importance of jointed rock mass for a geotechnical engineer, an effort has been made to predict the strength and deformation behaviour of jointed rock mass, by conducting tests on joints made up of model material in laboratory conditions. The objectives of present study are as follows:

- (i) Material property of plaster of paris and plaster of paris-sand mix
- (ii) Preparation of joint
- (iii) Conduct of experiment test
- (iv) Study of effect of joint orientation on strength and deformation behaviour of jointed rock.
- (v) Comparison of experimental result with the empirical formulae
- (vi) Development of prediction model.

**1.2 Organization of thesis:**

(i) Chapter-1 Introduction: A brief introduction has been given of jointed rock mass. Factors which influence the strength and deformation behaviour of jointed rock mass discussed. Objective of work also explained in this chapter.

(ii) Chapter-2 Literature review: A detailed literature review has been done to see the effect of

joint frequency and joint orientation angle on jointed rock mass.

(iii) Chapter-3 Laboratory investigation: Specimen of model material plaster of paris and plaster of paris-sand mix has been prepared and test under direct shear test and loading frame.

(iv) Chapter-4 Results and discussion: Jointed and intact specimen of model material tested under direct shear test and loading frame to obtain shear parameter and uniaxial compressive strength. Graph has been plotted between joint factor and uniaxial compressive strength ratio and also, between joint factor and elastic modulus ratio.

(v) Chapter-5 Development of prediction model: Regression analysis has been done and equation for weak rock mass has been proposed.

(vi) Conclusion: Conclusion of present study has been presented in this chapter

(vii) Scope of future work: Different parameter and unlike aspects of jointed rock mass which can be study in future are presented in this chapter

(viii) Reference: This study used many researcher literatures, the reference of them provided in this chapter

## Chapter-2

### Literature Review

Intact rock mass properties, discontinuities in jointed rock mass and the properties of the joints can be determined in the laboratory where as direct physical measurements of the properties of the rock mass are very costly as compared to laboratory study. Artificial anisotropy have been introduced and studied mainly as they have the advantage of being easily made and re-created. The anisotropic strength behaviour of rock mass as slates, gypsum and shale has been studied by a large number of investigators. Laboratory studies carried by many researchers show that many different failure modes are possible in jointed rock and that the internal distribution of stresses within a jointed rock mass can be extremely complex.

#### **Joint frequency:**

Thaweboon et al. (2016) determine the strength and deformability by making small-scale rock mass models and introduced different types of anisotropy with multiple joint sets and frequencies under confining stresses up to 12 MPa. Thaweboon et al. (2016) use sand stone as a model material. Thaweboon et al. (2016) carried out experimental work and performed triaxial test and uniaxial compressive strength test with model material (sand stone). It is found from the experimental data that the strength decrease with the increasing in joint frequency. It is also found that for one-joint set specimens the deformation moduli parallel to the joints show the highest values compared to those that are normal to the joints. This research has a limitation such as all strength criteria used can only predicted the strengths of the rock mass specimens under the confining stresses up to 12 MPa. Tiwari and Rao (2006) carried out number of experiment of uniaxial, triaxial and true triaxial on a jointed specimen of model materials made by sand and lime, test criteria was various angle of orientation joint. From the experiment they found that the deformation modulus of rock mass is influenced due to intermediate principal stress similar to enhancement in triaxial compressive strength. The modulus enhancement in rock mass with joint geometries corresponding to  $\Phi=40$  and  $60$  degrees is more than in case of joint geometries of  $\Phi=0, 20, 80$  and  $90$  degree. Thus, weak rocks are subjected to more modulus enhancement than comparatively harder rocks. Singh and Rao (2005) a large number of uniaxial compressive strength (UCS) tests were conducted on the specimens of jointed block mass having various combinations of orientations and different levels of interlocking of joints. Four dominating modes of failure were observed. The findings of the study have been verified by applying it to estimate the ultimate rock mass strength of nine rock types from few dam sites in the lower Himalayas. The ultimate strength obtained by the present methodology is compared with that obtained through the Q classification system. It is concluded that reasonably good estimates on field strength of jointed rocks are possible by using the correlations suggested in this study. Arora (1987) found that with increasing joint frequency strength of the material decreases. Lama (1974) performed many test to determine the influence of the number of the number of horizontal and vertical joints on strength. Lama (1974) conducted extensive tests on model material of different strength. Lama (1974) proposed the following equation based on his results:  $\sigma_c = K (L/l)^v$  Where,  $\sigma_c$  = compressive strength;  $K$  = strength of the specimen containing more than 150 joints;  $v$  = constant;  $L$  = length of the specimen; and  $l$  = length of the element.

#### **Joint orientation angle:**

Xin and Zhihong (2012) studied the deformation behaviour of jointed rock masses in uniaxial



compression by model materials with a set of pre-existing open joints. It was found that the two joint geometrical parameters, i.e., joint inclination angle and joint continuity factor, had great influence on the deformation behaviour of rock mass. It is also found by Xin and Zhihong (2012) that the ratio of residual strength to the maximum peak strength adopted a ductility index, and the first and the last peak strain were used as auxiliary parameters to investigate brittleness of the specimens. Singh et al. (2002) developed a link between strength and deformability of jointed block masses with the properties of intact specimens, obtained from simple laboratory tests, taking into account the influence of the properties of the joints. Singh et al. (2002) have done the experimental work and performed uniaxial compression test with the model material. Singh et al. (2002) use sand- lime brick as a model material. Singh et al. (2002) found that Strength and deformation behaviour of a jointed rock mass is a complicated phenomenon due to combinations of modes of failure. Singh et al. (2002) have given some empirical relation of strength of jointed specimen with the intact specimen ( $\sigma_{cj} = \sigma_{ci} e^{(a_j)}$ ) and also jointed modulus with the intact modulus ( $E_j = E_i e^{(b_j)}$ ). Jade and Sitharam (2003) studied statistical analysis of the uniaxial compressive strength and of the elastic modulus of jointed rock masses under different confining pressures. Properties of the rock masses with different joint fabric, with and without gouge have been considered in the analysis. A large amount of experimental data of jointed rock masses from the literature has been compiled and used for this statistical analysis. The uniaxial compressive strength of a rock mass has been represented in a non-dimensional form as the ratio of the compressive strength of the jointed rock to the intact rock. In the case of the elastic modulus, the ratio of elastic modulus of jointed rock to that of intact rock at different confining pressures is used in the analysis. The effect of the joints in the rock mass is taken into account by a joint factor. The joint factor is defined as a function of joint frequency, joint orientation, and joint strength. Several empirical relationships between the strength and deformation properties of jointed rock and the joint factor have been arrived at via statistical analysis of the experimental data. A comparative study of these relationships is presented. The effect of confining pressure on the elastic modulus of the jointed rock mass is also considered in the analysis. The study conclude that the jointed rock mass will act both as an elastic material and a discontinuous mass. The results obtained by the model with equivalent properties of the jointed rock mass predict fairly well the behavior of jointed rock mass.. Arora and Ramamurthy (1994) found that minimum strength of jointed rock mass found at 30° to 40°. Arora (1987) conducted uniaxial compressive strength test and triaxial test on intact and jointed specimens of rock mass. Arora (1987) used plaster of Paris, Jamarani sandstone , and Agra sandstone as model materials. Arora (1987)) conducted a large number of laboratory testing of intact specimen and jointed specimens to disclosed that the significant factors which influence the strength and modulus values of the jointed rock are frequency of joint, orientation of joints with respect to major principal stress direction, and strength of joint. On the based of results Arora (1987) gives a parameter which is called as joint factor ( $J_f$ ) and it is defined as,  $J_f = J_n / (n \cdot r)$  Where,  $J_n$  = number of joints per meter depth;  $n$  = inclination parameter depending on the orientation of the joint ;  $r$  = roughness parameter depending on the joint condition. Yaji (1984) performed triaxial tests on intact and single jointed specimens. Yaji

(1984) used plaster of Paris, sandstone, and granite the model materials. Yaji (1984) has also conducted tests on step-shaped and berm-shaped joints in plaster of Paris. Yaji (1984) presented the results in the form of failure envelopes and stress strain curves for different confining pressures. The modulus exponent (n) as well as modulus number (k) can be determined by the plots of modulus of elasticity versus confining pressure. The results of these experiments were analysed for strength and deformation purposes. It was found from the test results that the type of failure is dependent on couples of parameter such as confining stress and orientation of the joints. There are three mode of failure observed in the joint specimens with rough joint surface are: (i) By shearing across the joint, (ii) by tensile splitting (iii) by a combination of thereof.

### Failure modes in rock mass

Singh et al. (2002) the failure modes were identified based on the visual observations at the time of failure. The failure modes obtained are:

- (i) Splitting of intact material of the elemental blocks,
- (ii) Shearing of intact block material,
- (iii) Rotation of the blocks, and
- (iv) Sliding along the critical joints.

These modes were observed to depend on the combination of orientation  $n$  and the stepping. The angle  $\theta$  in this study represents the angle between the normal to the joint plane and the loading direction, whereas the stepping represents the level/extent of interlocking of the mass. The following observations were made on the effect of the orientation of the joints and their interlocking on the failure modes. These observations may be used as rough guidelines to assess the probable modes of failure under a uniaxial loading condition in the field.

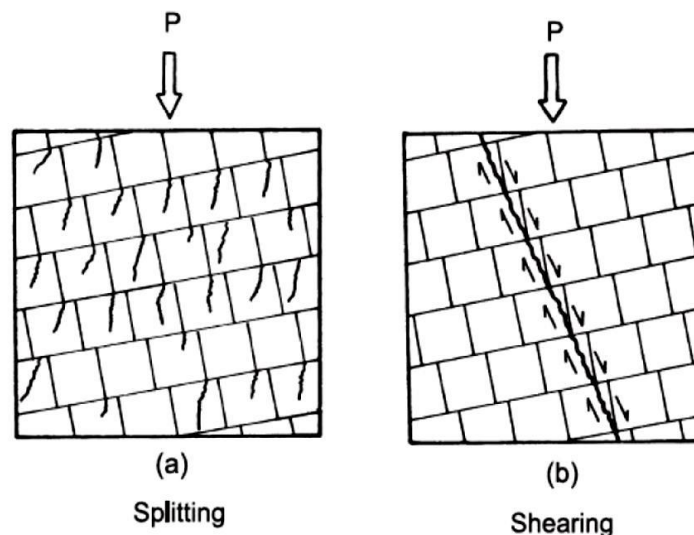


Figure 2.1: Splitting and shearing modes of failure (Singh et al.,2002)

#### (i) Splitting

Splitting failure is a type of failure in which material fails due to tensile stresses developed inside

the elemental blocks. The cracks are roughly vertical with no sign of shearing. This type of failure is observed in specimen when joints are either horizontal or vertical and are tightly interlocked due to stepping.

### (ii) Shearing

In shearing mode of failure, the specimen fails due to shearing of the elemental block material. In this mode of failure, The failure planes are inclined and are marked with signs of displacements and formation of fractured material along the sheared zones. This type of failure mode occurs when the continuous joints are close to horizontal (i.e.,  $\theta \leq 10^\circ$ ) and the mass is moderately interlocked.

The tendency to fail in shearing can be reduce by increase the angle  $n$ , and sliding takes place. For  $\theta \approx 30^\circ$ , shearing occurs only if the mass is highly interlocked due to stepping.

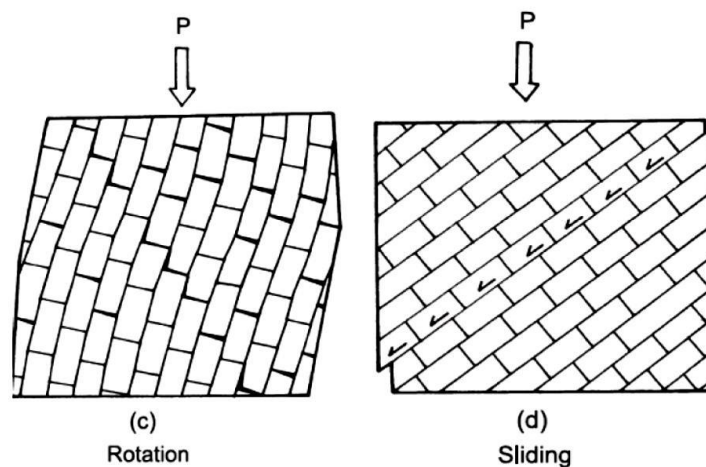


Figure 2.2: Rotation and sliding modes of failure (Singh et al., 2002)

### (iii) Sliding

In this mode of failure, the specimen fails due to sliding on the continuous joints. The mode is associated with large deformations, stick-slip phenomenon, and poorly defined peak in stress-strain curves. This mode of failure occurs in the specimen with joints inclined between  $\theta \approx 20^\circ - 30^\circ$  if the interlocking is nil or low. For orientations,  $\theta = 35^\circ - 65^\circ$  sliding occurs invariably for all the interlocking conditions.

### (iv) Rotation

In this mode of failure the rock mass fails due to rotation of the elemental blocks. It occurs for all interlocking conditions if the continuous joints have  $\theta > 70^\circ$ , except for  $\theta$  equal to  $90^\circ$  when splitting is the most possible way failure mode.

# Chapter-3 Laboratory investigation

## 3.1 Experimental Programme

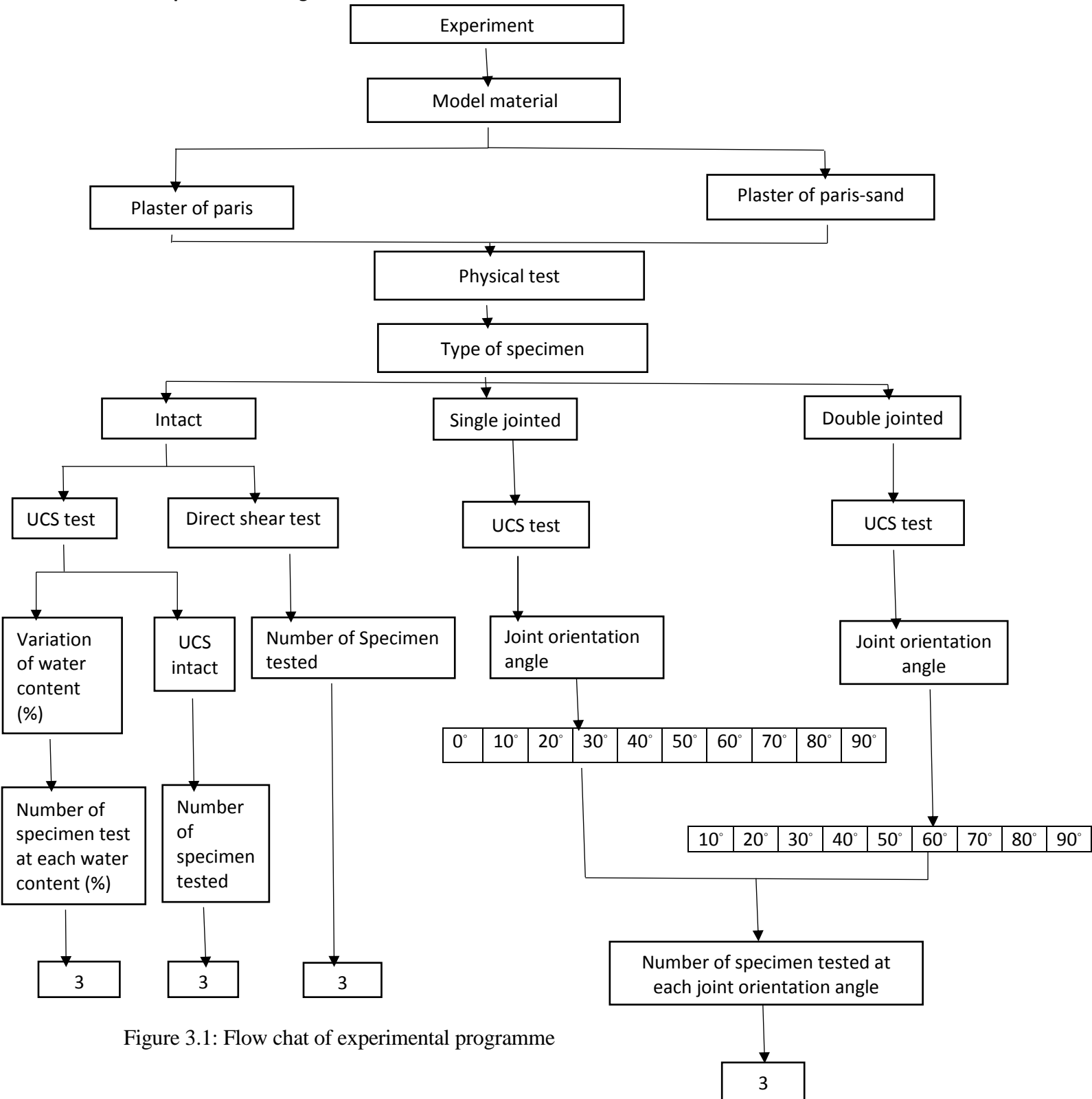


Figure 3.1: Flow chat of experimental programme

Experimental programme has been shown in the form of flow chart in figure 1.1. In this study, specimens were tested to obtain their uniaxial compressive strength, deformation behaviour and shear parameters. The tests conducted to obtain these parameters were direct shear test and uniaxial compression test. These tests were carried as per IS codes IS: 12634:1989 and IS: 9143:1979

### 3.1.1 Direct shear test:

The direct shear test was performed to determine (roughness factor) joint strength  $r = \tan \phi_j$  in order to predict the joint factor  $J_f$  (Arora 1987). Direct shear test was conducted on specimen of plaster of paris and plaster of paris – sand mix to know  $C_j$  and  $\phi_j$  values at 0.1 MPa, 0.2 MPa, and 0.3 MPa respectively. These tests were carried out on conventional direct shear test apparatus shown in figure 3.1.1 as per IS code (IS: 12634:1989).



Figure 3.1.1: Direct shear test

### 3.1.2 Uniaxial compressive strength test:

In Uniaxial Compressive Strength test the cylindrical specimens were subjected to major principal stress till the rock mass specimen failure. In this test the samples were fixed to cylindrical shape, length in the ratio of 2 to 3 times the diameter the ends maintained flat within 0.02mm. Perpendicularity of the axis were not deviated by 0.001radian. The prepared specimens having dimension  $L=76$  mm &  $D=38$  mm were put in between the two steel plates of the testing machine and load applied at the predetermined rate along the axis of the sample till the sample fails.

The deformation of the specimen was measured with the help of a separate dial gauge. During the test, load versus deformation readings were taken and a graph is plotted. When a brittle type of failure occurs, the proving ring dial indicates a definite maximum load which drops quickly with the further increase of strain. At failure the applied load was noted. The load is divided by the bearing surface of the specimen which gives the uniaxial compressive strength of the specimen.

Uniaxial compressive strength tests were conducted on intact specimens, jointed specimens with single and double joints to know the strength as well as the deformation behaviour of intact and jointed rocks. Failure of intact specimen under compression shown in the figure 3.1.4. The specimens were tested for different orientation angles such as 0, 10, 20, 30, 40, 50, 60, 70, 80, 90 degrees and for intact specimens (shown in figure 3.1.5 and 3.1.6). For each orientation of joints, three U.C.S tests were conducted as shown in the table 3.1.1 and table 3.1.2. The jointed specimens were placed inside a rubber membrane before testing of U.C.S to avoid slippage along the joints just after application of the load (shown in figure 3.1.3). These tests were carried out on conventional loading frame (CBR test machine) shown in figure 3.1.2 as per IS code (IS: 9143: 1979)



Figure 3.1.2: Uniaxial compression test for intact rock specimen





Figure 3.1.3: Uniaxial compression test for jointed rock specimen





Figure 3.1.4: Failure of intact specimen

**Table 3.1.1:** Uniaxial compression test (single joint)

Types of joints	1J-0°	1J-10°	1J-20°	1J-30°	1J-40°	1J-50°	1J-60°	1J-70°	1J-80°	1J-90°
No. of jointed specimen tested	3	3	3	3	3	3	3	3	3	3

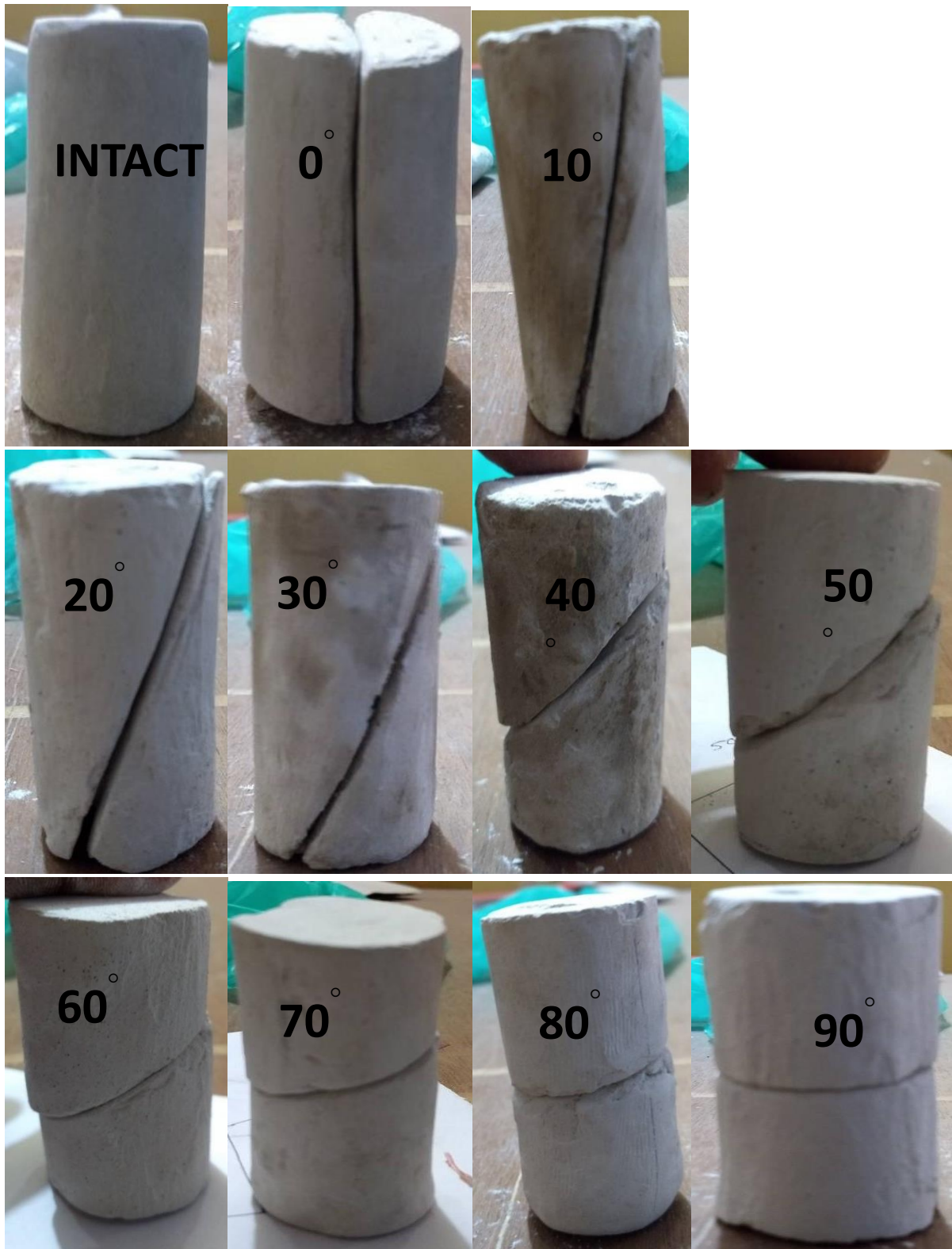


Fig. 3.1.5: Types of joints studied in plaster of paris specimens and sand- plaster of paris mix specimens (single jointed specimens are shown here)

**Table 3.1.2:** Uniaxial compression test (double joint):

<b>Types of joints</b>	2J-0°	2J-10°	2J-20°	2J-30°	2J-40°	2J-50°	2J-60°	2J-70°	2J-80°	2J-90°
<b>No. of jointed specimen tested</b>	0	3	3	3	3	3	3	3	3	3



Figure 3.1.6: Types of joints studied in plaster of paris specimens and sand- plaster of paris mix specimens (double jointed specimens are shown here)

### 3.2 Materials used:

Experiments have been conducted on model materials to get uniform, identical or homogenous specimen in order to understand the failure mechanism, strength and deformation behaviour of jointed rock mass. It is observed that plaster of paris has been used as model material to simulate weak rock mass in the field. Many investigators have used plaster of paris because of its ease in casting, flexibility, instant hardening, low cost, easy availability and joint can be easily create. Numerous type of anisotropy can be introduce plaster of Paris. And in the field sand is the one of the composition of many soft rock materials. To obtained strength and deformed abilities in relation to actual rocks has made by Plaster of Paris and sand is one of the suitable material for preparation a soft rock model in geotechnical engineering and hence it is used to prepare models for this investigation.

### 3.3 Model of the specimens:

Two types of model materials (specimen) prepared.

- 1) Plaster of paris
- 2) Plaster of paris and sand mix
  - I. Type of mould is cylindrical (L/D ratio=2)
  - II. On the basis of trial proportion of POP and fine sand by weight will be considered are as follows.
  - III. The ratio of plaster of paris and sand is 8:2 (POP: sand = 8:2)
  - IV. Size of each specimen (L/D = 2:1) D = 38 mm and L = 76 mm.
  - V. Water quantity has been considered as per the OMC determinations.

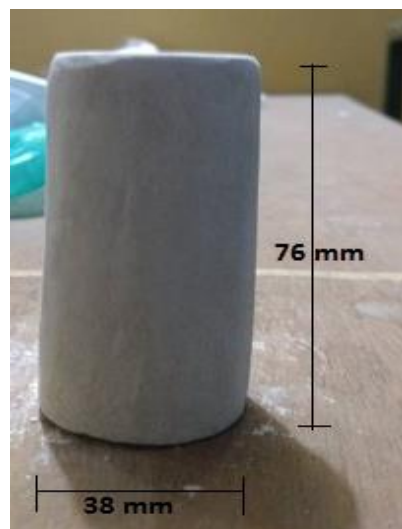


**Figure 3.3.1:** Dimension of specimen

### **3.4 Preparation of specimens**

Plaster of Paris is procured from the local market and Yamuna sand were used. Plaster of Paris powder is produced by pulverizing partially burnt gypsum which is duly white in color with smooth feel of cement. The water content at which maximum density is to be achieved is found out by conducting number of trial tests with different percentage of water. The optimum moisture content was found out to be 30% and 29% by weight for POP & POP-sand mix specimens respectively. For preparation of Plaster Of Paris specimen, 132 gm of plaster of Paris is mixed thoroughly with 39.6 cc (30% by weight) water and for Plaster Of Paris-sand mixture specimen, 135 gm of materials (sand-29 gm. +POP-106 gm.) is mixed thoroughly with 39.15 cc (29% by weight) water to form a uniform paste. The specimens are prepared by pouring the plaster mix in the mould and vibrating for approximately 2 min for proper compaction and to avoid presence of air gaps. After that it is allowed to set for 5 min. and after hardening, the specimen was extruded manually from the mould by using an extruder. The specimens are polished by using sand paper. The polished specimens are then kept for air dry for 7 days.

### **3.5 Curing**

Specimen is air dry for 7 days. Before testing each specimen of Plaster of Paris obtaining constant weight dimensioned to  $L/D = 2:1$ , at  $L = 76$  mm,  $D = 38$  mm.

### **3.6 Making joints in specimens**

There are following instruments which are used in making joints in specimen

- 1) Light weight hammer
- 2) Blade
- 3) Scale
- 4) Pencil
- 5) Protractor

Two longitudinal lines are drawn on the specimen just opposite to each other. At the center of the line the desired orientation angle is marked with the help of a protractor. Then this marked specimen is placed on the table and with the help blade cutting along the drawn line, hammered continuously to break along the line. It is observed that the joints thus formed comes under a category of rough joint. The uniaxial compressive strength test and direct shear test are performed on the intact specimens, jointed specimens with single and double joints to know the strength as well as deformation behaviour of intact and jointed rocks and the shear parameters respectively.



## Chapter - 4

### Results and discussions

#### 4.1 Direct shear test results:

The roughness parameter ( $r$ ) which is the tangent value of the friction angle ( $\Phi_j$ ) was found from the direct shear test performed at different normal stresses. The variation of shear stress with normal stress for rock mass specimens tested in direct shear tests are illustrated in the fig.: 4.1.1 and their corresponding values are given in the table 4.1.1. The value of cohesion ( $C_j$ ) for jointed specimens of Plaster of Paris has been found as 0.178 MPa and for plaster of paris and sand mixture it has been found as 0.182. Value of friction angle ( $\Phi_j$ ) for plaster of paris and plaster of paris-sand found as  $39^\circ$  and  $41^\circ$  respectively. The roughness parameter ( $r = \tan\Phi_j$ ) found to be 0.809 for the specimens of Plaster of Paris (P.O.P) tested and for plaster of paris-sand mix it is found to be 0.869 .

**Table 4.1.1:** Values of shear stress for different values of normal stress on specimens of plaster of paris in direct shear stress test.

Cross sectional area of samples =  $3600\text{mm}^2$

Normal stress, $\sigma_n$ (MPa)	Shear stress, $\tau$ (MPa)
0.049	0.298
0.098	0.417
0.147	0.537

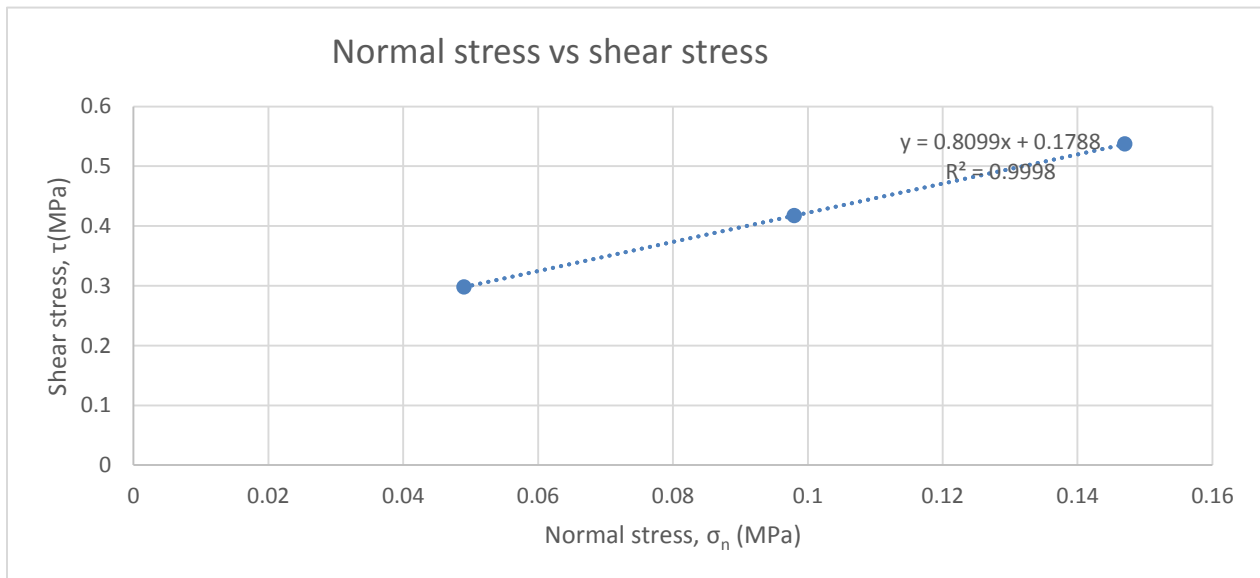


Figure 4.1.1: Normal stress vs shear stress (Plaster of paris)

**Table 4.1.2:** Values of shear stress for different values of normal stress on specimens of plaster of paris-sand mixture in direct shear stress test.

Cross sectional area of samples = 3600mm<sup>2</sup>

Normal stress, $\sigma_n$ (MPa)	Shear stress, $\tau$ (MPa)
0.049	0.328
0.098	0.462
0.147	0.581

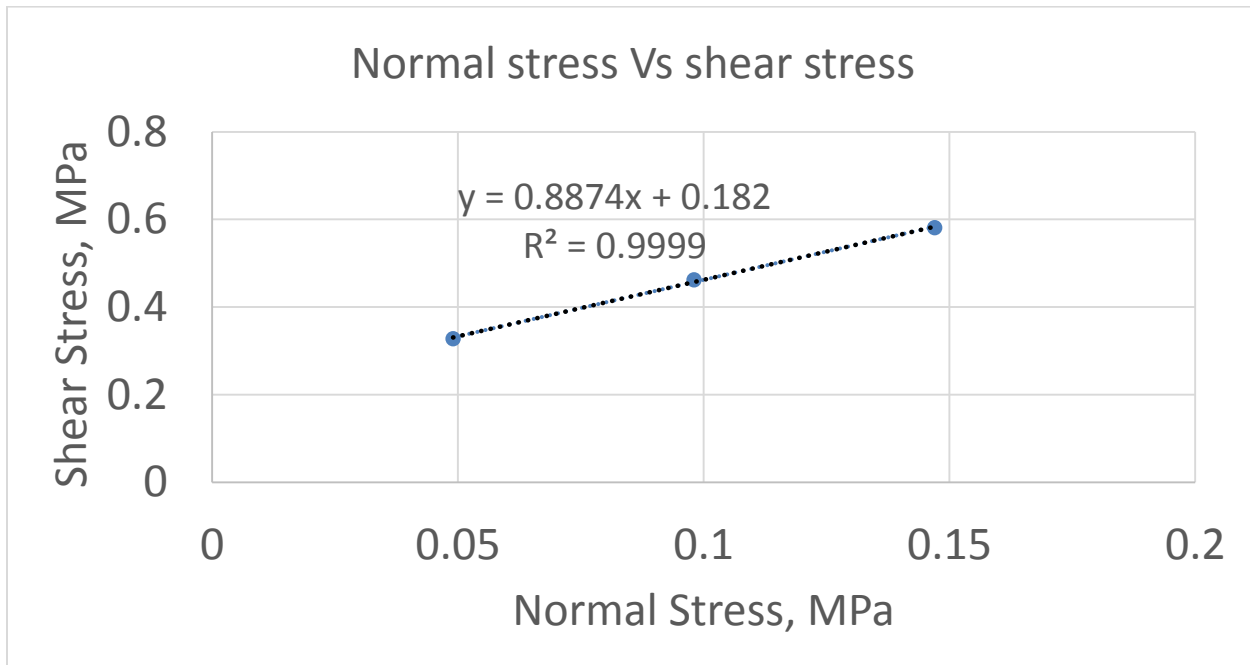


Figure 4.1.2: Normal stress vs shear stress (Plaster of paris-sand mix)

## 4.2 Uniaxial compression test results:

### 4.2.1 Intact Specimen of plaster of paris

The variation of stress as obtained in uniaxial compression test for the intact specimen of Plaster of Paris for different values of water content is illustrated below:

**Table 4.2.1:** Uniaxial compressive strength (MPa) values against water content (%) for plaster of paris.

<b>Water Content (%)</b>	25	27	28	30	32	34	35
<b>Uniaxial compressive strength(MPa)</b>	8.52	9.10	9.57	10.12	9.60	9.20	8.55



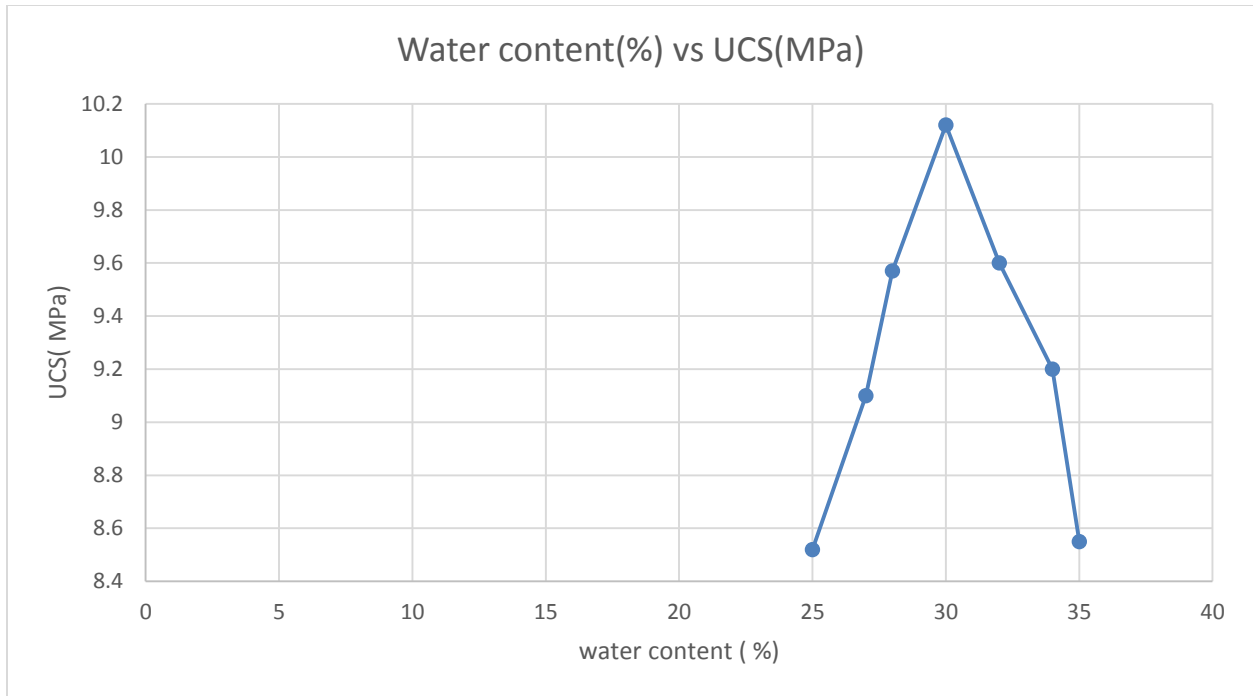


Figure 4.2.1 Water content Vs Uniaxial compressive strength (plaster of paris)

The optimum value of uniaxial compressive strength ( $\sigma_{ci}$ ) evaluated from the above test was found to be 10.12 MPa.

### Intact specimen

The variation of stress as obtained in uniaxial compression test for the intact specimen of Plaster of Paris-sand mix for different values of water content is illustrated below:

**Table 4.2.2:** Uniaxial compressive strength (MPa) values against water content (%) for plaster of paris- sand mix

Water content (%)	24	26	27	29	31	33	34
Uniaxial compressive strength(MPa)	9.10	9.52	10.20	10.87	10.16	9.20	8.10

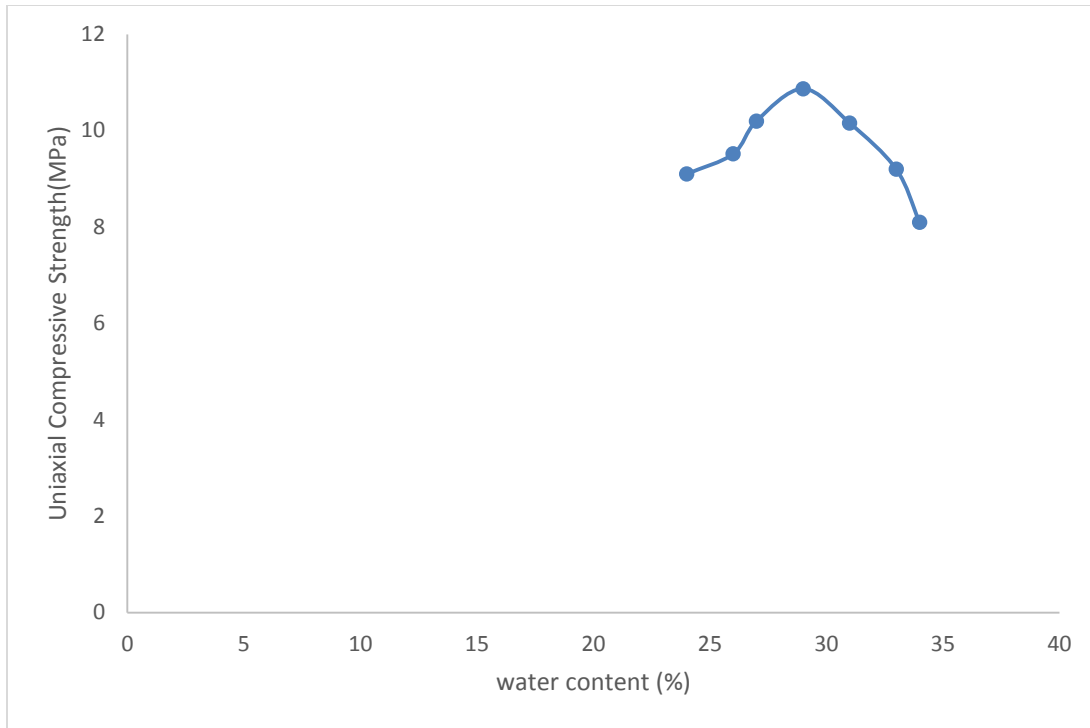


Figure 4.2.2: Water content (%) Vs uniaxial compressive strength (MPa) (plaster of paris-sand mix)

**For intact specimens:**

**Plaster of paris:**

The variations of the stress with strain as obtained in uniaxial compression test for the intact specimen of plaster of paris is illustrated in the fig.4.2.3 and its corresponding stress vs strain values are presented in table 4.2.3. The value of uniaxial compression strength ( $\sigma_i$ ) evaluated from the above tests was found to be 10.12 MPa. The modulus of elasticity of intact specimen ( $E_{ti}$ ) has been calculated at 50% of the  $\sigma_i$  value to account the tangent modulus. The value of  $E_{ti}$  was found as  $0.340 \times 10^3$  MPa.

**Table 4.2.3:** Values of stress and strain for intact specimens:

- Length of specimen = 76mm
- Diameter of specimen = 38mm
- Cross sectional area of the specimen = 1134 mm<sup>2</sup>
- Strain rate = 0.5 mm/minute

Axial strain, $\epsilon_a$ (%)	Uniaxial compressive strength, $\sigma_{ci}$ (MPa)
0	0
0.658	2.53
1.316	4.46
1.974	5.95
2.631	8.31
3.289	9.91
3.421	10.12
4.605	10.02

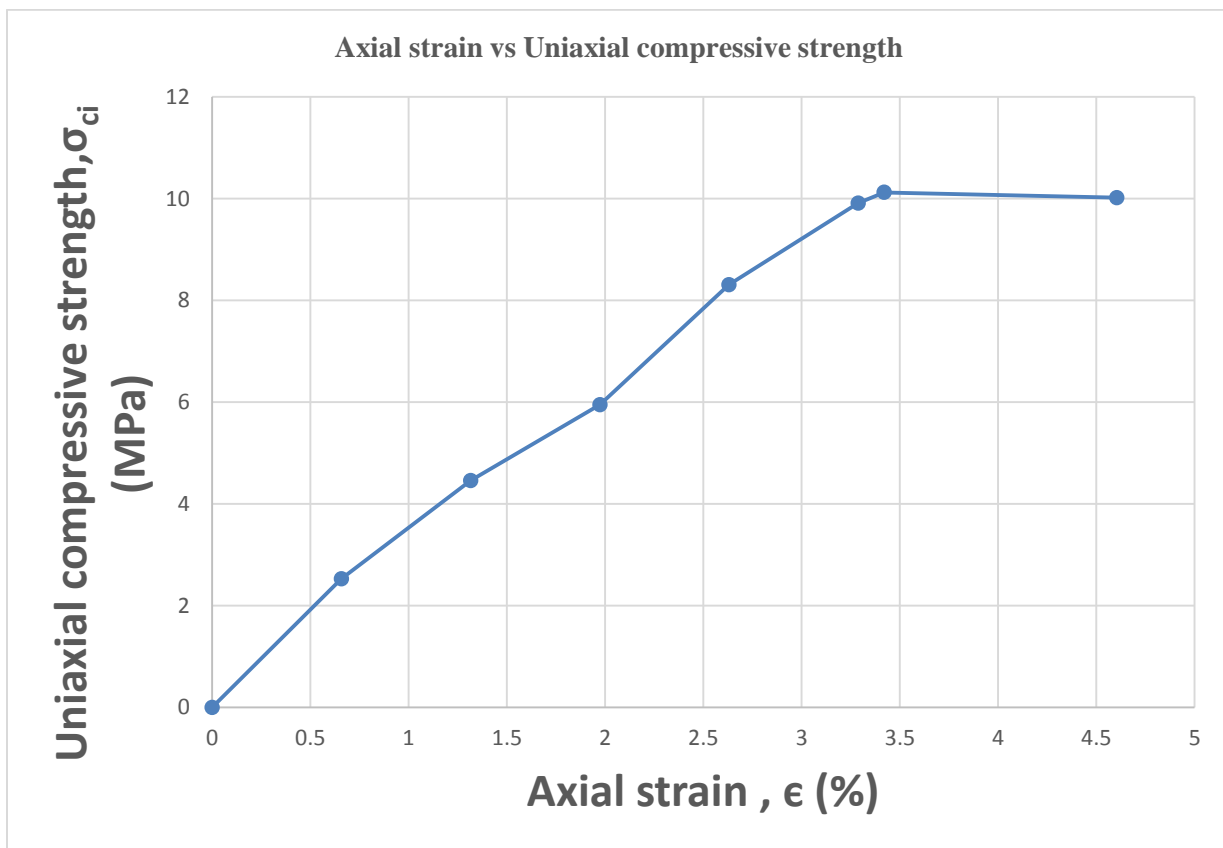


Figure 4.2.3: Stress-strain curve (Plaster of paris)

**Plaster of paris-sand mix:**

The variations of the stress with strain as obtained in uniaxial compression test for the intact specimen of plaster of paris is illustrated in the fig. 4.2.4 and its corresponding stress vs strain values are presented in table 4.2.4. The value of uniaxial compression strength ( $\sigma_{ci}$ ) evaluated from the above tests was found to be 10.87 MPa. The modulus of elasticity of intact specimen ( $E_{ti}$ ) has been calculated at 50% of the  $\sigma_i$  value to account the tangent modulus. The value of  $E_{ti}$  was found as  $0.360 * 10^3$  MPa.

**Table 4.2.4:** Uniaxial Compressive strength (MPa) and axial strain (%)

<b>Axial strain, <math>\epsilon_a</math>(%)</b>	<b>Uniaxial compressive strength, <math>\sigma_{ci}</math> (MPa)</b>
0	0
0.658	2.75
1.316	4.24
1.974	6.167
2.631	8.31
3.289	9.91
3.421	10.87
4.605	10.77
5.263	10.56

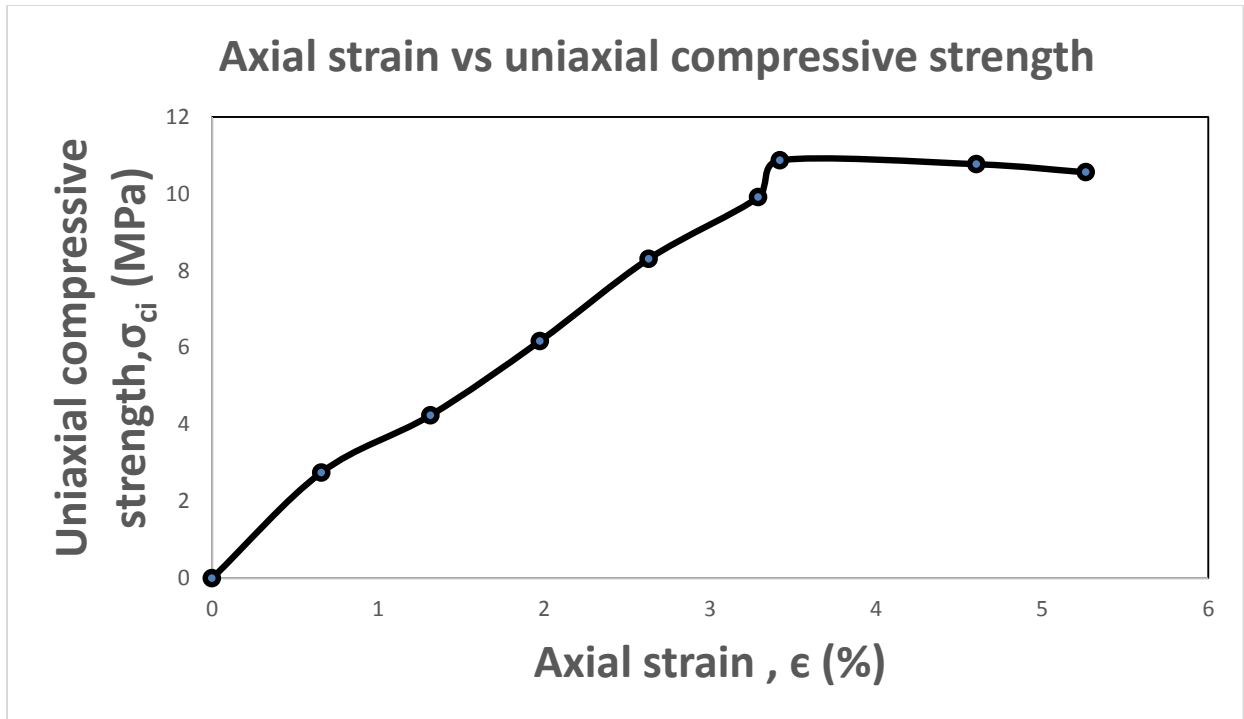


Figure 4.2.4: stress-strain curve (Plaster of paris- sand mixture)

**Table: 4.2.5** Orientation angle ( $\beta^\circ$ ) vs uniaxial compressive strength,  $\sigma_{cj}$  (MPa) of plaster Of paris jointed specimen:

Orientation angle ( $\beta^\circ$ )	Uniaxial compressive strength, $\sigma_{cj}$ (MPa)
0	7.730
10	7.410
20	4.670
30	2.420
40	3.810
50	6.920
60	7.560
70	7.880
80	8.090
90	9.160

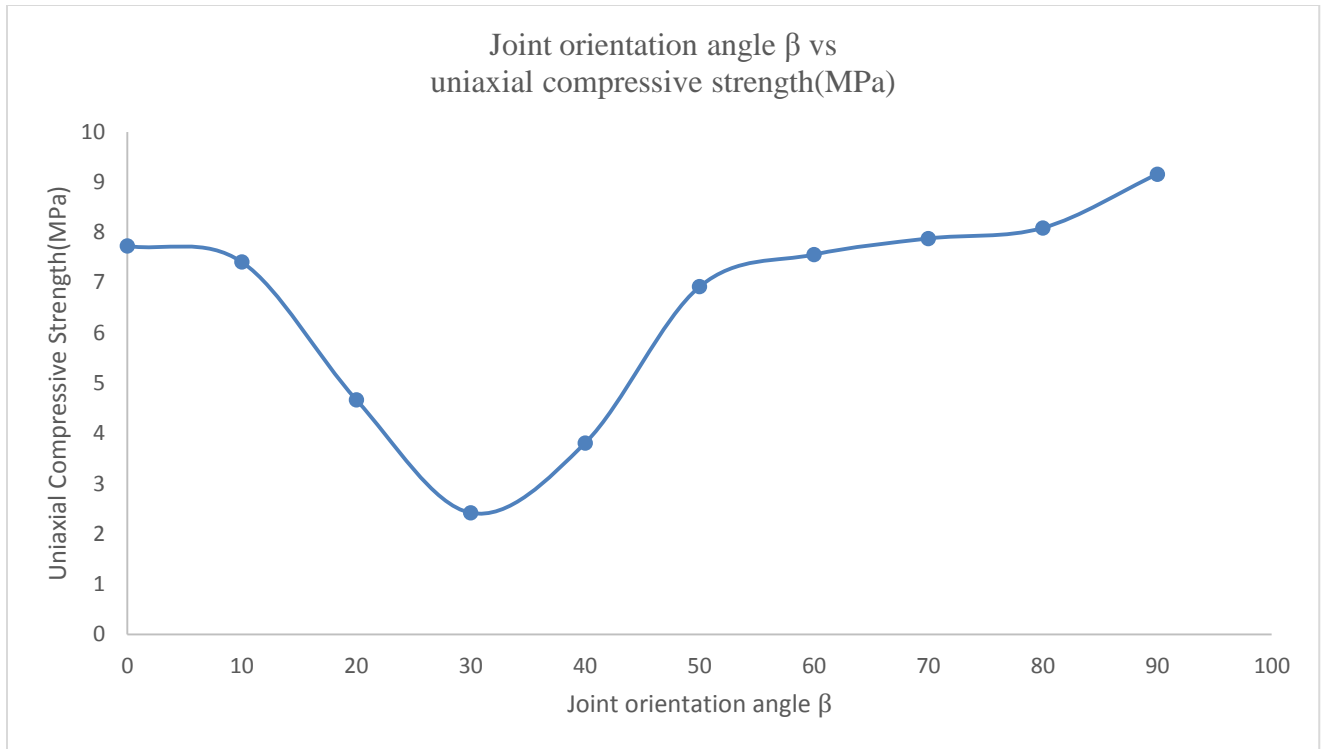


Figure 4.2.5: Joint orientation angle  $\beta$  vs uniaxial compressive strength (MPa)

**Table: 4.2.6** Orientation angle ( $\beta^\circ$ ) vs uniaxial compressive strength,  $\sigma_{cj}$  (MPa) of plaster of paris- sand mix jointed specimen:

Orientation angle ( $\beta^\circ$ )	Uniaxial compressive strength, $\sigma_{cj}$ (MPa)
0	8.53
10	7.73
20	4.46
30	2.64
40	4.24
50	6.6
60	7.56
70	8.95
80	9.59
90	10.02

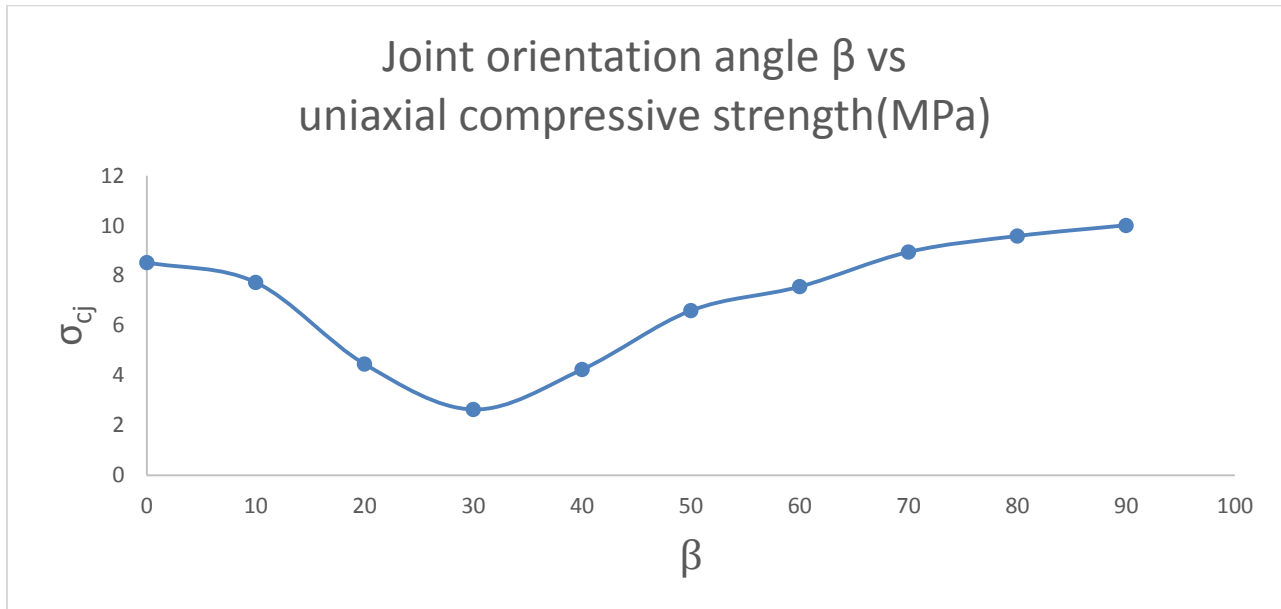


Figure 4.2.6: Joint orientation angle  $\beta$  vs uniaxial compressive strength(MPa)

#### 4.3 Parameter Studied:

**Table 4.3.1** Physical and engineering properties of plaster of paris used for joints studied:

S. No.	Property/Parameter	Values
1	Uniaxial compressive strength, $\sigma_{ci}$ (MPa)	10.12
2	Tangent modulus, ( $E_{ti}$ ) (MPa)	340
3	Cohesion intercept, $C_j$ (MPa)	0.178
4	Angle of friction, $\Phi_j$ (degree)	39°

**Table 4.3.2** Physical and engineering properties of plaster of paris – sand mix used for joints studied:

S. No.	Property/Parameter	Values
1	Uniaxial compressive strength, $\sigma_{ci}$ (MPa)	10.87
2	Tangent modulus, ( $E_{ti}$ ) (MPa)	360
3	Cohesion intercept, $C_j$ (MPa)	0.182
4	Angle of friction, $\Phi_j$ (degree)	41°

#### 4.4 Comparison of results with the empirical formulae for jointed specimen of plaster of paris and sand-plaster of paris mix

##### Strength criteria

The uniaxial compressive strength (UCS) of intact specimens obtained from the test results has been found out. Also, the uniaxial compressive strength ( $\sigma_{cj}$ ) as well as modulus of elasticity ( $E_{ij}$ ) for the jointed specimens was calculated after testing the jointed specimens. For testing of jointed specimen, the jointed specimens are placed inside a rubber membrane before testing, to avoid slippage along the critical joints. After obtaining the values of ( $\sigma_{cj}$ ) and  $E_{ij}$  for different orientations ( $\beta$ ) of joints, it was perceived that the jointed specimens show minimum strength when the joint orientation angle was at  $30^\circ$  and maximum when angle was  $90^\circ$ . The values of ( $\sigma_{cr}$ ) for different orientation angle ( $\beta$ ) were obtained with the help of the following relationship:

$$\sigma_{cr} = \sigma_{cj} / \sigma_{ci}$$

The values of joint factor ( $J_f$ ) were evaluated by using the relationship:

$$J_f = J_n / (n * r)$$

Arora (1987) has suggested the following relationship between  $J_f$  and  $\sigma_{cr}$  as,

$$\sigma_{cr} = e^{-0.008 * J_f}$$

Arora (1987) has suggested the following relationship between  $J_f$  and  $E_r$  as,

$$E_r = e^{-0.0115 * J_f}$$

Padhy (2005) has suggested the following relationship between  $J_f$  and  $\sigma_{cr}$  as,

$$\sigma_{cr} = e^{-0.09 * J_f}$$

Padhy (2005) has suggested the following relationship between  $J_f$  and  $E_r$  as,

$$E_r = e^{-0.0125 * J_f}$$



**Table 4.4.1:** Values of  $J_n$ ,  $J_f$ ,  $\sigma_{cj}$ ,  $\sigma_{cr}$  for jointed specimen of plaster of paris (Single joint):

Joint type in degrees	$J_n$	$n$	$r = \tan\Phi_j$	$J_f = J_n/(n*r)$	$\sigma_{cj}$ (MPa)	Present study $\sigma_{cr} = \sigma_{cj}/\sigma_{ci}$	Predicted Arora(1987) $\sigma_{cr} = e^{-0.008*J_f}$	Predicted Padhy (2005) $\sigma_{cr} = e^{-0.09 *J_f}$
0	13	0.810	0.809	19.839	7.730	0.764	0.853	0.168
10	13	0.460	0.809	34.933	7.410	0.731	0.756	0.043
20	13	0.105	0.809	153.040	4.670	0.460	0.294	$10^{-06}$
30	13	0.046	0.809	349.331	2.420	0.398	0.061	0000
40	13	0.071	0.809	226.327	3.810	0.375	0.163	0000
50	13	0.306	0.809	52.514	6.920	0.684	0.656	0.009
60	13	0.465	0.809	34.557	7.560	0.746	0.756	0.045
70	13	0.634	0.809	25.346	7.880	0.779	0.816	0.102
80	13	0.814	0.809	19.741	8.090	0.798	0.854	0.169
90	13	1.000	0.809	16.069	9.160	0.904	0.878	0.235

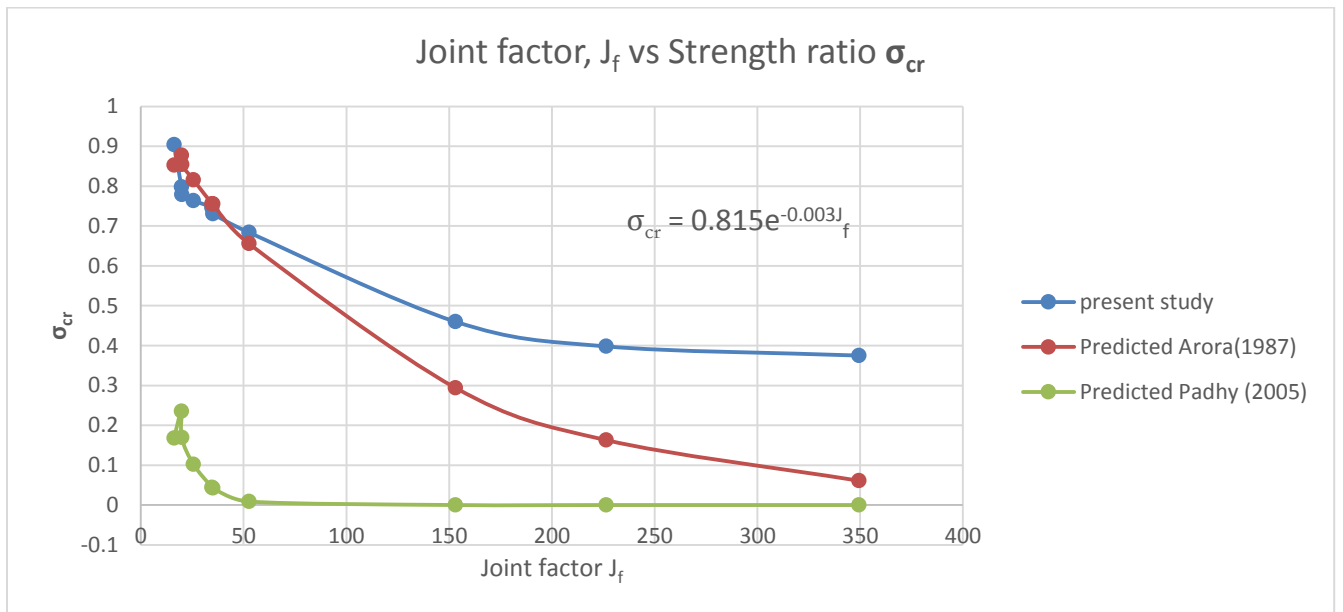


**Figure 4.4.1:** Joint factor,  $J_f$  vs strength ratio  $\sigma_{cr}$  (single jointed)

**Table 4.4.2:** Values of  $E_{tj}$ ,  $E_r$ ,  $J_n$ , and  $J_f$  for jointed specimens of plaster of paris (Single joint)

Joint type in degrees	$J_n$	$n$	$r = \tan\Phi_j$	$J_f = J_n/(n*r)$	$E_{tj}$ (MPa)	Present study $E_r = E_{tj}/E_{ti}$	Predicted Arora(1987) $E_r = e^{-0.0115*J_f}$	Predicted Padhy (2005) $E_r = e^{-0.0125*J_f}$
0	13	0.810	0.809	19.839	271	0.797	0.796	0.780
10	13	0.460	0.809	34.933	267.3	0.785	0.668	0.646
20	13	0.105	0.809	153.040	102.3	0.300	0.172	0.148
30	13	0.046	0.809	349.331	21.4	0.050	0.018	0.013
40	13	0.071	0.809	226.327	68	0.200	0.074	0.059
50	13	0.306	0.809	52.514	183	0.538	0.545	0.519
60	13	0.465	0.809	34.557	209	0.614	0.672	0.649
70	13	0.634	0.809	25.346	214	0.629	0.747	0.727
80	13	0.814	0.809	19.741	242	0.712	0.797	0.781
90	13	1.000	0.809	16.069	292.96	0.850	0.831	0.818

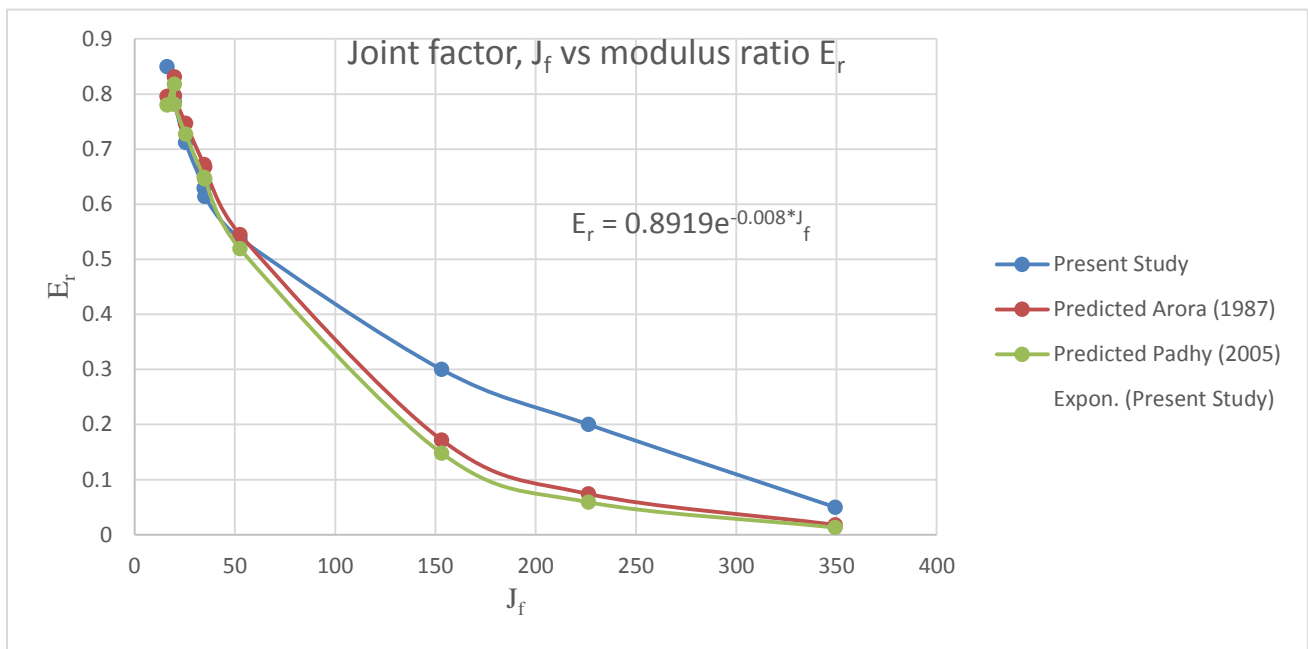
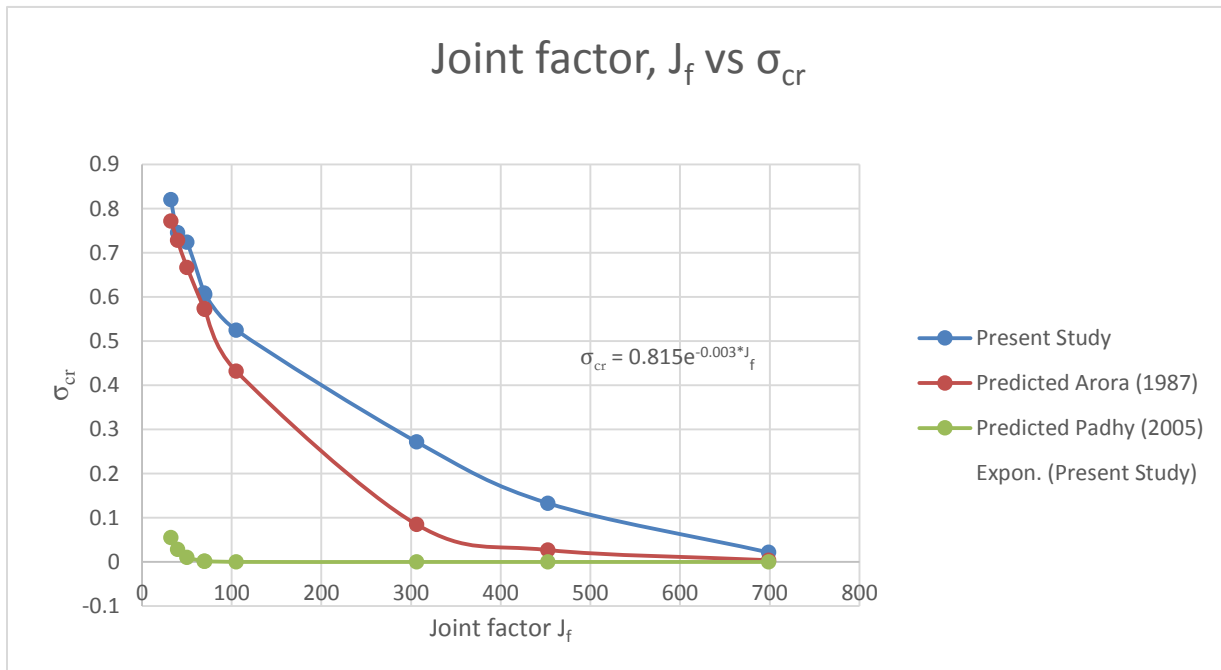


Figure 4.4.2: Joint factor,  $J_f$  vs modulus ratio  $E_r$  (single jointed)

**Table 4.4.3:** Values OF  $J_n$ ,  $J_f$ ,  $\sigma_{cj}$ ,  $\sigma_{cr}$  for plaster of paris jointed specimens (double joint)

Joint type in degrees	$J_n$	$n$	$r = \tan\Phi_j$	$J_f = J_n/(n*r)$	$\sigma_{cj}$ (MPa)	Present study $\sigma_{cr} = \sigma_{cj}/\sigma_{ci}$	Predicted Arora(1987) $\sigma_{cr} = e^{-0.008*J_f}$	Predicted Padhy (2005) $\sigma_{cr} = e^{-0.09*J_f}$
10	26	0.460	0.809	69.866	6.130	0.606	0.572	0.002
20	26	0.105	0.809	306.080	2.750	0.272	0.085	0
30	26	0.046	0.809	698.662	1.140	0.113	0.004	0
40	26	0.071	0.809	452.654	2.210	0.217	0.027	0
50	26	0.306	0.809	105.028	5.310	0.525	0.432	8E-05
60	26	0.465	0.809	69.115	6.170	0.609	0.574	0.002
70	26	0.634	0.809	50.692	7.340	0.724	0.667	0.01
80	26	0.814	0.809	39.482	7.560	0.746	0.728	0.029
90	26	1.000	0.809	32.138	8.310	0.820	0.772	0.055



**Figure 4.4.3:** Joint factor,  $J_f$  vs strength ratio  $\sigma_{cr}$  (double jointed)

**Table 4.4.4:** Values OF  $E_{tj}$  ,  $E_r$ ,  $J_n$  and  $J_f$  for plaster of paris jointed specimens (double joints)

Joint type in degrees	$J_n$	$n$	$r = \tan\Phi_j$	$J_f = J_n/(n*r)$	$E_{tj}$ (MPa)	Present study $E_r = E_{tj}/E_{ti}$	Predicted Arora(1987) $E_r = e^{-1.15*10^{-2} * J_f}$	Predicted Padhy (2005) $E_r = e^{-1.25*10^{-2} * J_f}$
10	26	0.460	0.809	69.866	225	0.623	0.448	0.418
20	26	0.105	0.809	306.080	63	0.174	0.03	0.022
30	26	0.046	0.809	698.662	18.46	0.051	3E-04	2E-04
40	26	0.071	0.809	452.654	27.44	0.076	0.006	0.004
50	26	0.306	0.809	105.028	96.73	0.268	0.299	0.269
60	26	0.465	0.809	69.115	171.13	0.474	0.452	0.422
70	26	0.634	0.809	50.692	196	0.543	0.558	0.531
80	26	0.814	0.809	39.482	199	0.551	0.635	0.611
90	26	1.000	0.809	32.138	269	0.745	0.691	0.669

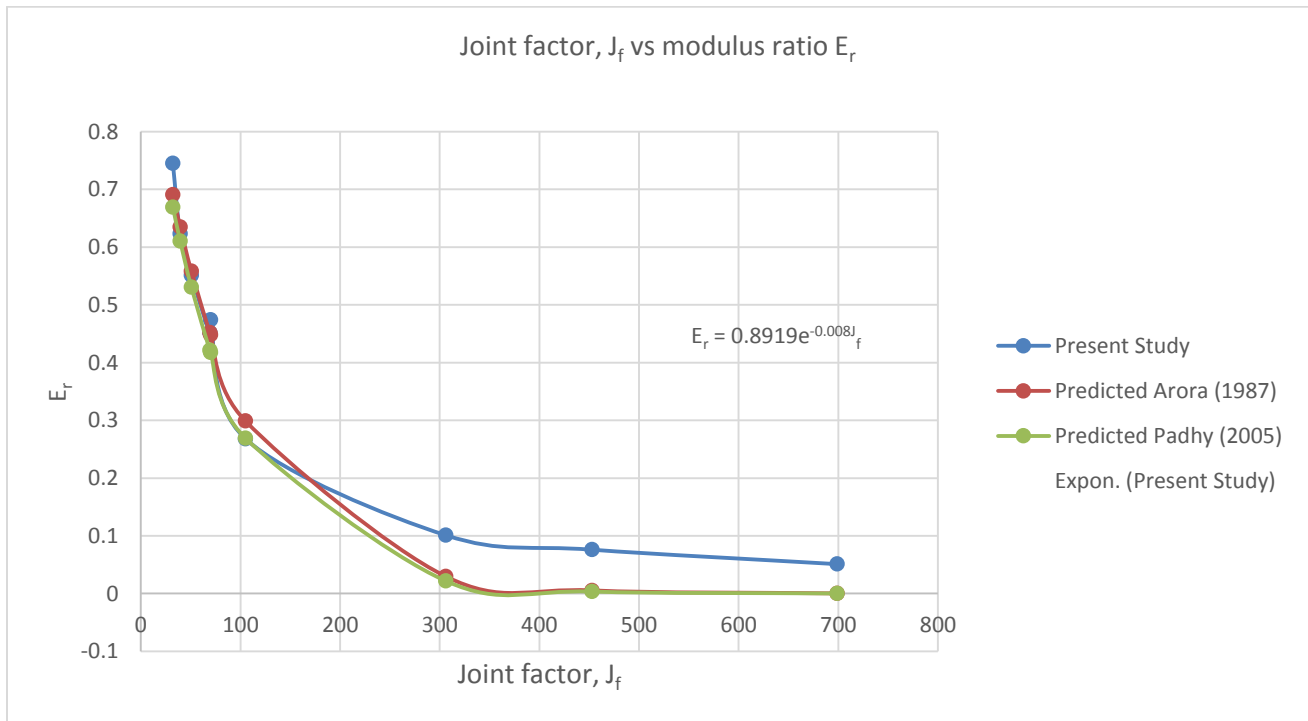


**Figure 4.4.4:** Joint factor,  $J_f$  vs modulus ratio  $E_r$  (double jointed)

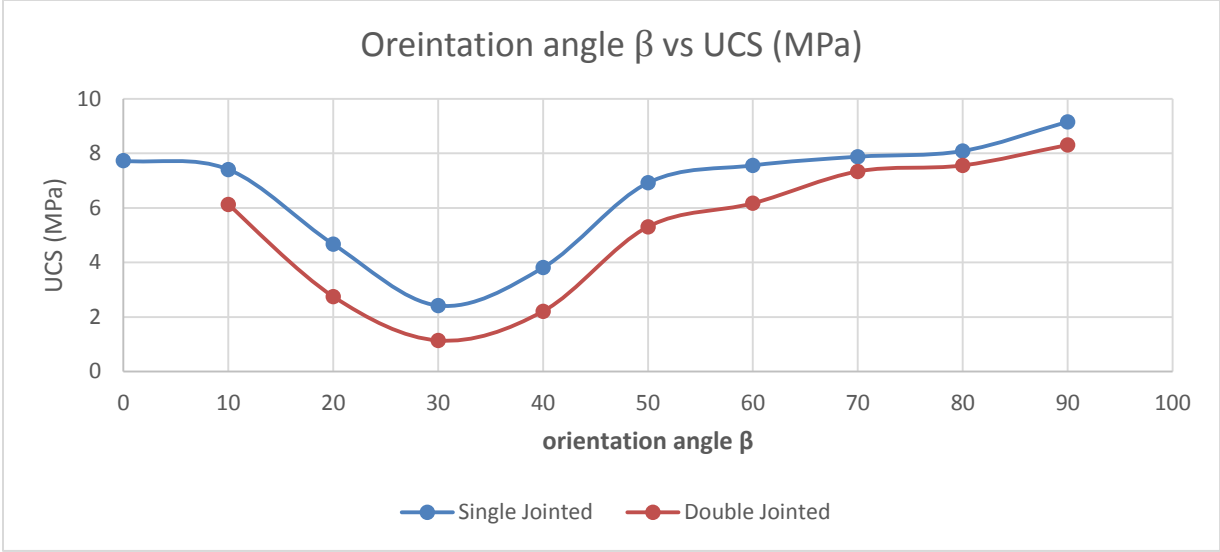
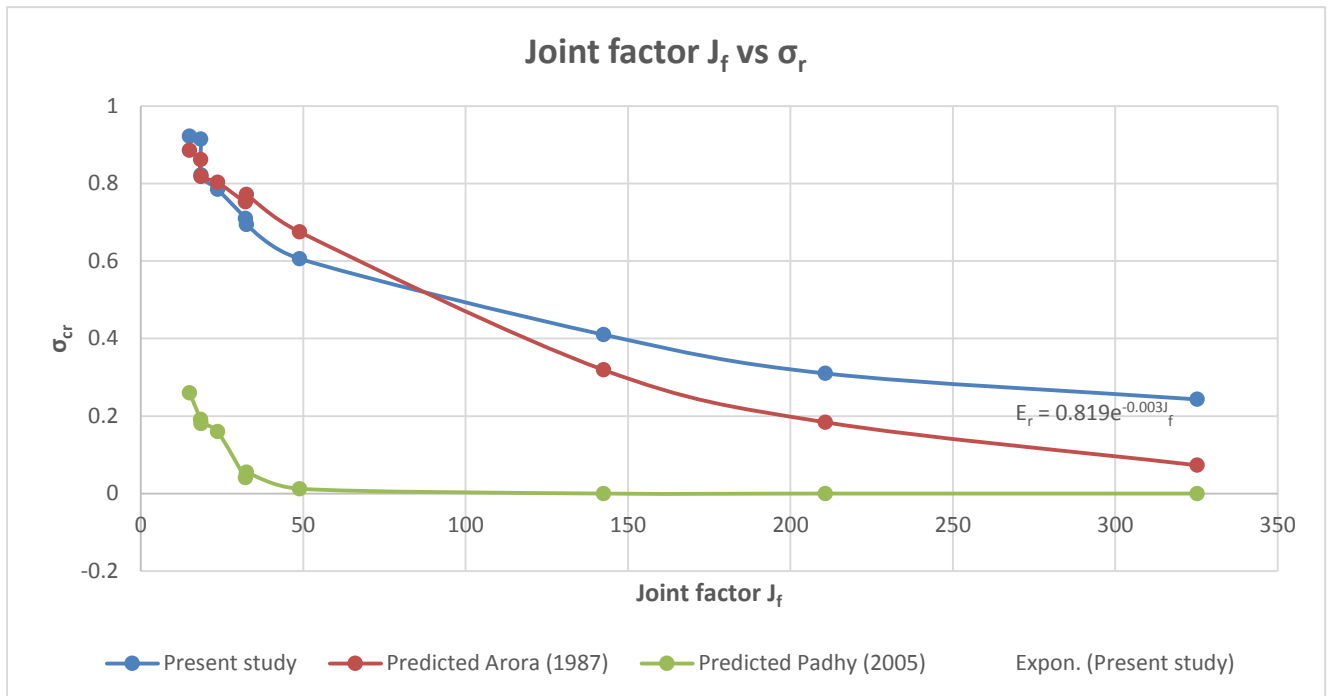


Figure 4.4.5: Comparison of single jointed and double jointed orientation angle  $\beta$  (plaster of paris)

**Table 4.4.5:** Values of  $J_n$ ,  $J_f$ ,  $\sigma_{cj}$ ,  $\sigma_{cr}$  for jointed specimens of sand- plaster of paris mixture (Single joint)

Joint type in degrees	$J_n$	$n$	$r = \tan\Phi_j$	$J_f = J_n/(n*r)$	$\sigma_{cj}$ (MPa)	Present Study $\sigma_{cr} = \sigma_{cj}/\sigma_{ci}$	Predicted Arora(1987) $\sigma_{cr} = e^{-0.008*J_f}$	Predicted Padhy (2005) $\sigma_{cr} = e^{-0.09*J_f}$
0	13	0.810	0.869	18.469	8.53	0.785	0.863	0.190
10	13	0.460	0.869	32.521	7.73	0.710	0.753	0.041
20	13	0.105	0.869	142.474	4.46	0.410	0.319	0000
30	13	0.046	0.869	325.211	2.64	0.243	0.073	0000
40	13	0.071	0.869	210.700	4.24	0.390	0.184	0000
50	13	0.306	0.869	48.888	6.6	0.606	0.675	0.012
60	13	0.465	0.869	32.171	7.56	0.694	0.772	0.055
70	13	0.634	0.869	23.596	8.95	0.822	0.828	0.120
80	13	0.814	0.869	18.378	9.59	0.915	0.862	0.191
90	13	1.000	0.869	14.960	10.02	0.922	0.886	0.260



**Figure 4.4.6:** Joint factor  $J_f$  vs strength ratio  $\sigma_r$  (single jointed)

**Table 4.4.6:** Values OF  $E_{tj}$  ,  $E_r$ ,  $J_n$  and  $J_f$  for jointed specimens of sand – plaster of paris mixture (single joint)

Joint type in degrees	$J_n$	$n$	$r = \tan\Phi_j$	$J_f = J_n/(n*r)$	$E_{tj}$ (MPa)	Present study $E_r = E_{tj}/E_{ti}$	Predicted Arora(1987) $E_r = e^{-0.0115*J_f}$	Predicted Padhy (2005) $E_r = e^{-0.0125*J_f}$
0	13	0.810	0.869	18.469	279	0.775	0.809	0.794
10	13	0.460	0.869	32.521	256	0.710	0.688	0.666
20	13	0.105	0.869	142.474	85	0.237	0.193	0.167
30	13	0.046	0.869	325.211	24	0.05	0.024	0.016
40	13	0.071	0.869	210.700	70	0.067	0.089	0.072
50	13	0.306	0.869	48.888	181	0.503	0.569	0.543
60	13	0.465	0.869	32.171	219	0.607	0.691	0.669
70	13	0.634	0.869	23.596	247	0.685	0.761	0.744
80	13	0.814	0.869	18.378	284	0.789	0.808	0.795
90	13	1.000	0.869	14.960	305	0.846	0.842	0.828

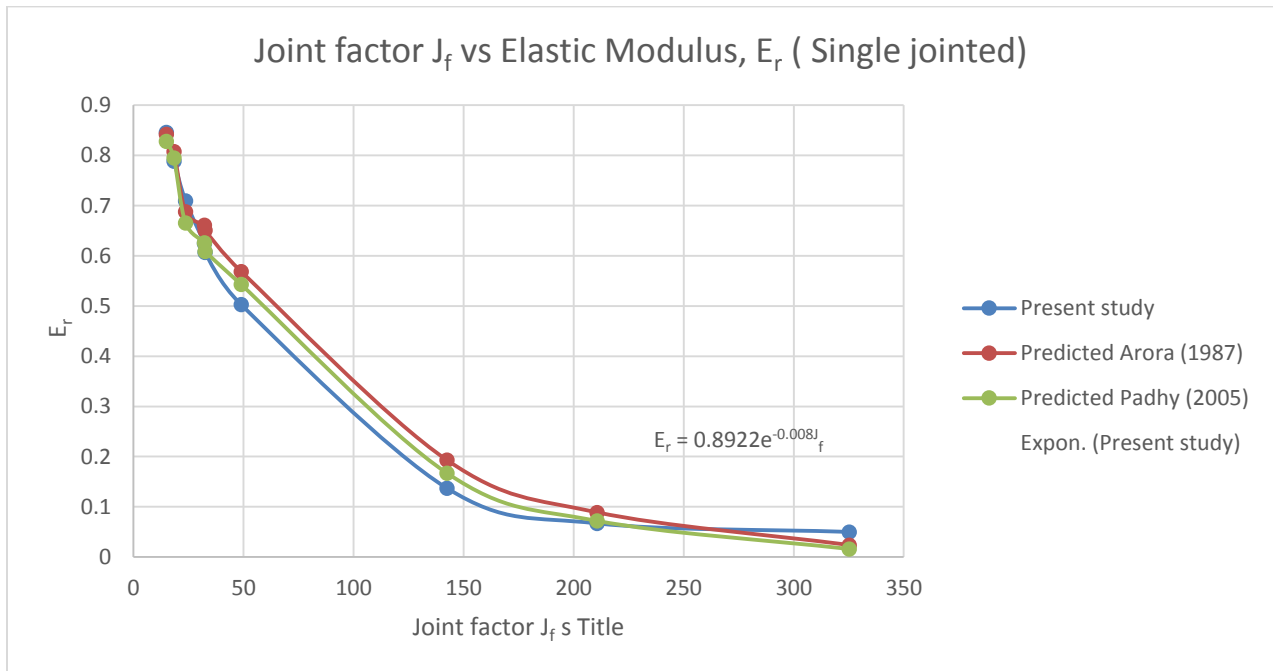


**Figure 4.4.7:** Joint factor  $J_f$  vs elastic modulus  $E_r$  (Single jointed)

**Table 4.4.7:** Values of  $J_n$ ,  $J_f$ ,  $\sigma_{cj}$ ,  $\sigma_{cr}$  for jointed specimen of sand- plaster of paris mix (double joint)

Joint type in degrees	$J_n$	$n$	$r = \tan\Phi_j$	$J_f = J_n/(n*r)$	$\sigma_{cj}$ (MPa)	Present Study $\sigma_{cr} = \sigma_{cj}/\sigma_{ci}$	Predicted Arora(1987) $\sigma_{cr} = e^{-0.008*J_f}$	Predicted Padhy (2005) $\sigma_{cr} = e^{-0.09*J_f}$
10	26	0.460	0.869	65.042	6.62	0.608	0.593	0.003
20	26	0.105	0.869	284.947	2.64	0.243	0.101	0000
30	26	0.046	0.869	650.423	2.1	0.192	0.005	0000
40	26	0.071	0.869	421.401	2.75	0.253	0.033	0000
50	26	0.306	0.869	97.776	5.41	0.498	0.456	1E-04
60	26	0.465	0.869	64.776	6.17	0.568	0.595	0.003
70	26	0.634	0.869	47.192	7.56	0.694	0.685	0.014
80	26	0.814	0.869	36.756	8.52	0.784	0.744	0.037
90	26	1.000	0.869	29.919	8.84	0.812	0.786	0.068

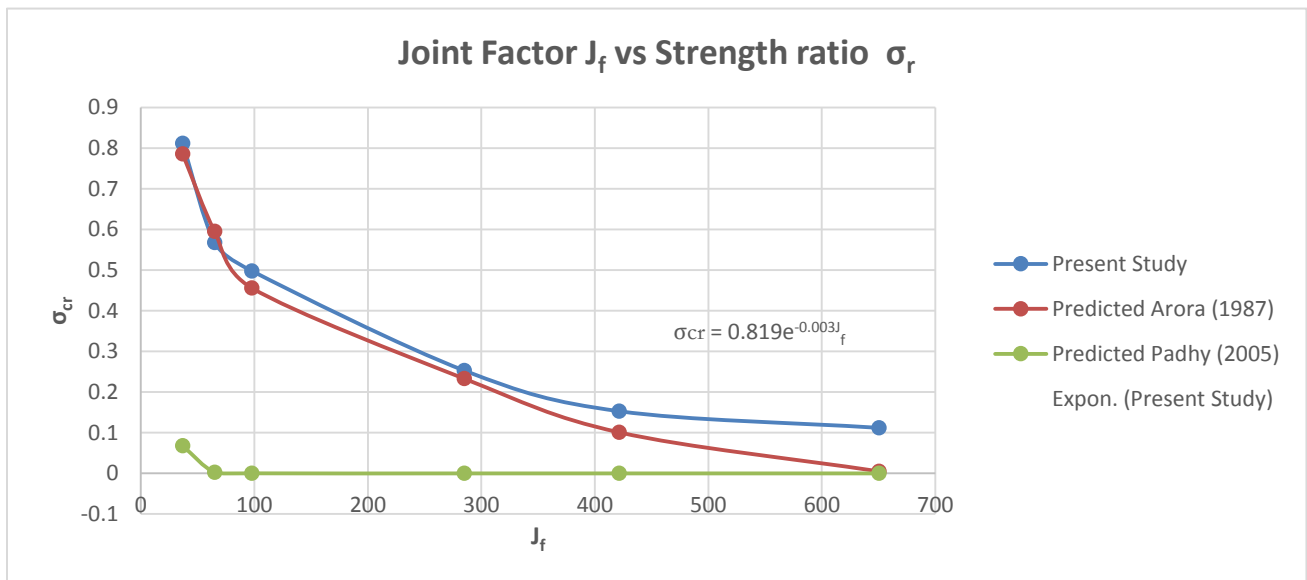
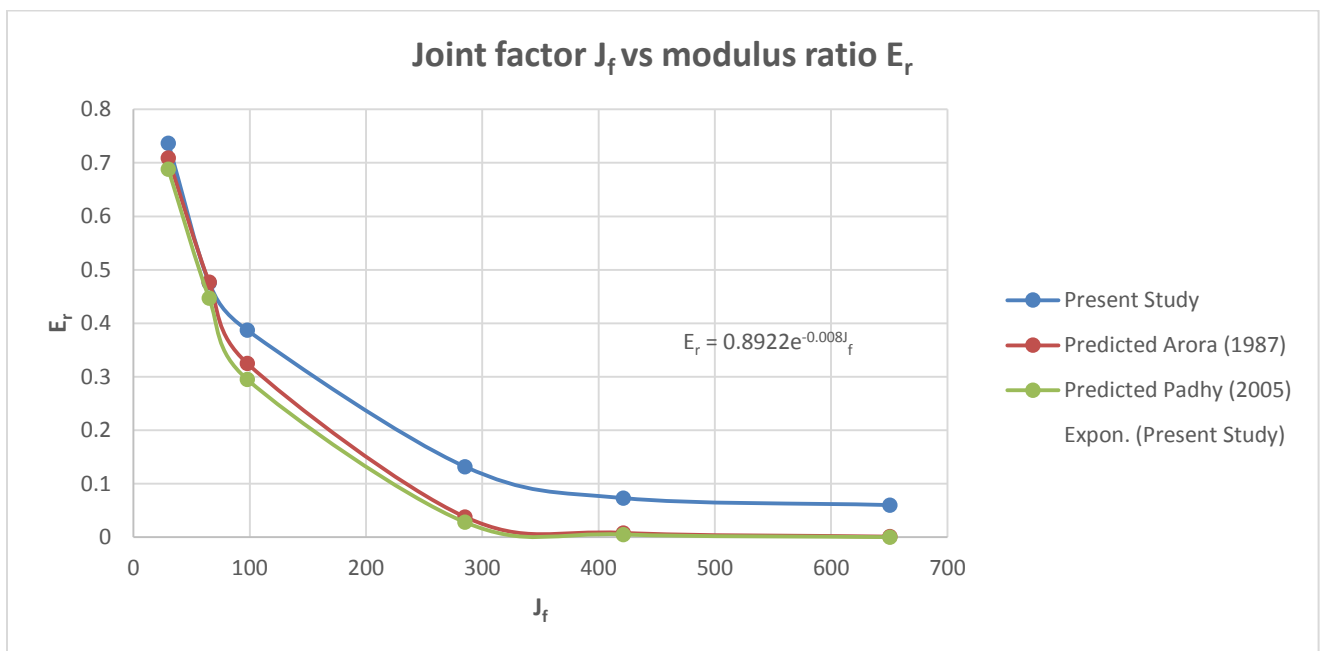


Figure 4.4.8: Joint Factor  $J_f$  vs Strength ratio  $\sigma_r$  (double Jointed)



**Table 4.4.8:** Values of  $E_{tj}$ ,  $E_r$ ,  $J_n$  and  $J_f$  for specimen of sand-plaster of paris mix (double joints)

Joint type in degrees	$J_n$	$n$	$r = \tan\Phi_j$	$J_f = J_n/(n*r)$	$E_{tj}$ (MPa)	Present Study $E_r = E_{tj}/E_{ti}$	Predicted Arora(1987) $E_r = e^{-0.0115 * J_f}$	Predicted Padhy (2005) $E_r = e^{-0.0125 * J_f}$
10	26	0.460	0.869	65.042	250.86	0.623	0.473	0.444
20	26	0.105	0.869	284.947	53.37	0.132	0.038	0.028
30	26	0.046	0.869	650.423	24.16	0.060	0.001	0.000
40	26	0.071	0.869	421.401	49.62	0.123	0.008	0.005
50	26	0.306	0.869	97.776	155.76	0.387	0.325	0.295
60	26	0.465	0.869	64.776	191.93	0.476	0.477	0.447
70	26	0.634	0.869	47.192	223.07	0.554	0.581	0.554
80	26	0.814	0.869	36.756	277.89	0.690	0.655	0.632
90	26	1.000	0.869	29.919	296.98	0.737	0.709	0.688



**Figure 4.4.9:** Joint factor  $J_f$  vs modulus ratio  $E_r$  (double jointed)

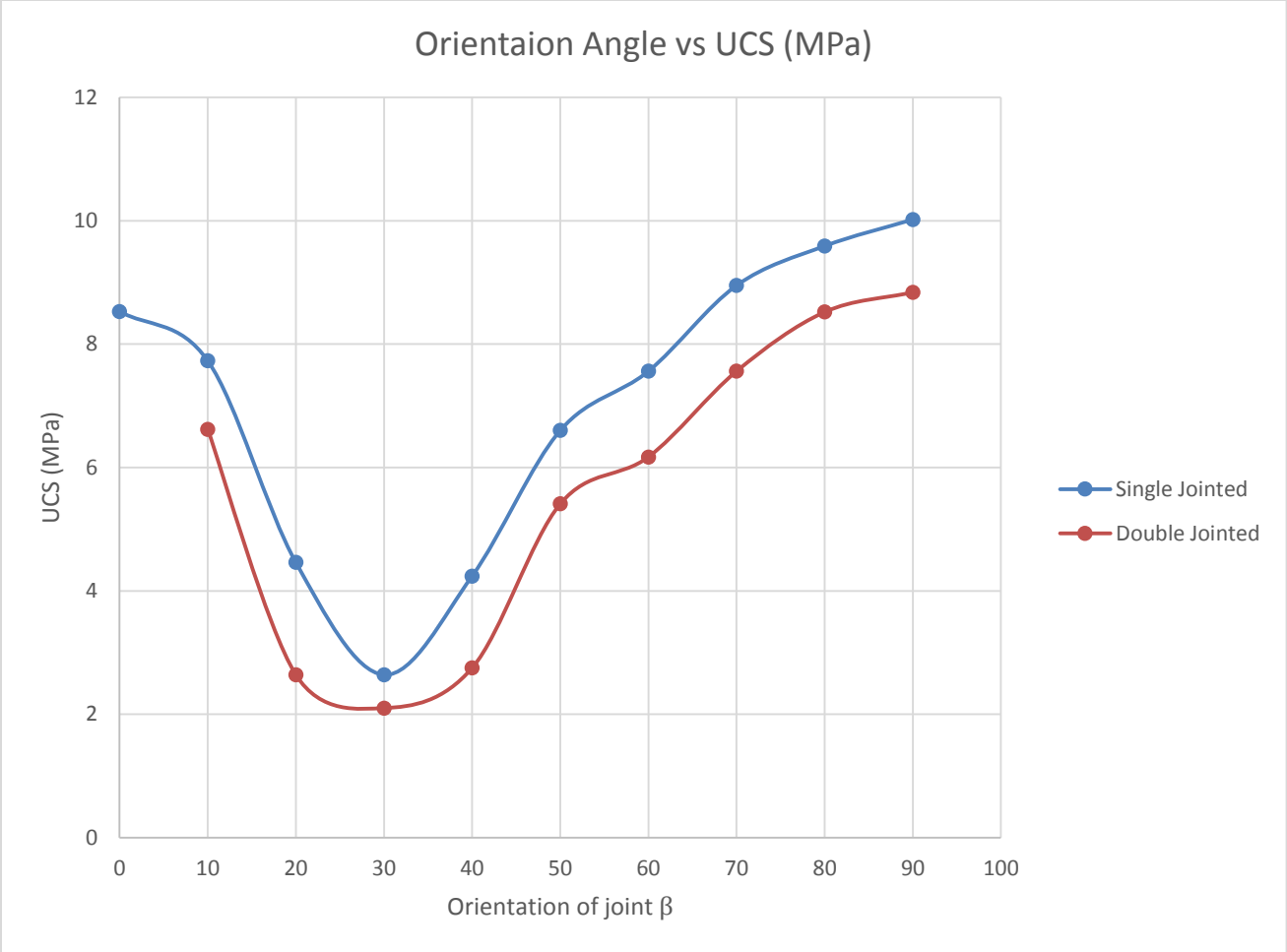


Figure 4.4.10: Comparison of Orientation Angle  $\beta$  of single and double Jointed specimen of Sand- plaster of paris mix

## Chapter-5

### Development of prediction model

The uniaxial compressive strength and elastic modulus ( $E_{ti}$ ) of intact specimen of plaster of Paris is found to be 10.12 MPa and  $0.340 \times 10^3$  MPa respectively. Therefore, as per ISRM (1979) classification of intact rocks, the plaster of Paris tested in this study is classified as low strength rock. And according to Deere and Miller (1966) classification as EL depicting very low strength and low modulus ratio. Also, The uniaxial compressive strength and elastic modulus ( $E_{ti}$ ) of intact specimen of plaster of Paris-sand mix is found to be 10.87 MPa and  $0.360 \times 10^3$  MPa respectively. Hence, as per ISRM (1979) classification of intact rocks, the plaster of Paris-sand mix tested in this study is classified as low strength rock. And according to Deere and Miller (1966) classification as EL depicting very low strength and low modulus ratio. Both the specimen plaster of Paris and plaster of Paris sand mix classify as very low strength rock.

Based on the basis of experimental results regression analysis has been done. And it is observed that uniaxial compressive strength ratio vary exponentially with joint factor, for both plaster of Paris and plaster of Paris-sand mix specimen. The variation of uniaxial compressive strength ratio with joint factor for both the sample are presented in equation (i) and (ii)

$$\sigma_{cr} = 0.815 e^{-0.003*J_f} \quad (\text{equation for plaster of Paris specimen}) \dots(i)$$

$$\sigma_{cr} = 0.819 e^{-0.003*J_f} \quad (\text{equation for plaster of Paris-sand specimen}) \dots(ii)$$

These two equations are approximately the same. Graph between joint factor and uniaxial compressive strength ratio for the single jointed specimen of plaster of Paris and plaster of Paris-sand mix and also, for double jointed specimen of plaster of Paris and plaster of Paris-sand mix shows that 0.815 and -0.003 is a constant factor with some approximation.

So, with some approximation we suggest this equation for low strength rock:

$$\sigma_{cr} = a e^{b*J_f} \quad \dots(iii)$$

where, a and b are constants.

$J_f$  is joint factor

$\sigma_{cr}$  is Uniaxial compressive strength ratio

a = 0.815

b = -0.003

Based on the basis of experimental results regression analysis has been done. And it is observed that elastic modulus ratio vary exponentially with joint factor, for both plaster of Paris and plaster of Paris-sand mix specimen. The variation of uniaxial compressive strength ratio with joint factor for both the sample are presented in equation (iv) and (v)

$$E_r = 0.8919 e^{-0.008 * J_f} \quad (\text{equation for plaster of paris specimen}) \dots (\text{iv})$$

$$E_r = 0.8922 e^{-0.008 * J_f} \quad (\text{equation for plaster of paris-sand specimen}) \dots (\text{v})$$

These two equations are approximately the same. Graph between joint factor and elastic modulus ratio for the single jointed specimen of plaster of paris and plaster of paris-sand mix and also for double jointed specimen of plaster of paris and plaster of paris-sand mix shows that 0.892 and -0.008 is a constant factor with some approximation.

So, with some approximation we suggest this equation for low strength rock:

$$E_r = a e^{b * J_f} \quad \dots (\text{vi})$$

Where, a and b are constants.

$J_f$  is joint factor

$E_r$  is elastic modulus ratio

$$a = 0.892$$

$$b = -0.008$$

**Table 5.1:** Comparison of uniaxial compressive strength ratio of prediction model with present study and empirical formulae (jointed specimen of plaster of paris, Single joint):

Joint factor, $J_f$	Present study $\sigma_{cr} = \sigma_{cj} / \sigma_{ci}$	Predicted Arora(1987) $\sigma_{cr} = e^{-0.008 * J_f}$	Predicted Padhy (2005) $\sigma_{cr} = e^{-0.09 * J_f}$	Prediction model $\sigma_{cr} = 0.815 e^{-0.003 * J_f}$
19.839	0.764	0.853	0.168	0.768
34.933	0.731	0.756	0.043	0.734
153.040	0.460	0.294	$10^{-6}$	0.515
349.331	0.398	0.061	0	0.286
226.327	0.375	0.163	0	0.413
52.514	0.684	0.656	0.009	0.696
34.557	0.746	0.756	0.045	0.735
25.346	0.779	0.816	0.102	0.755
19.741	0.798	0.854	0.169	0.768
16.069	0.904	0.878	0.235	0.777

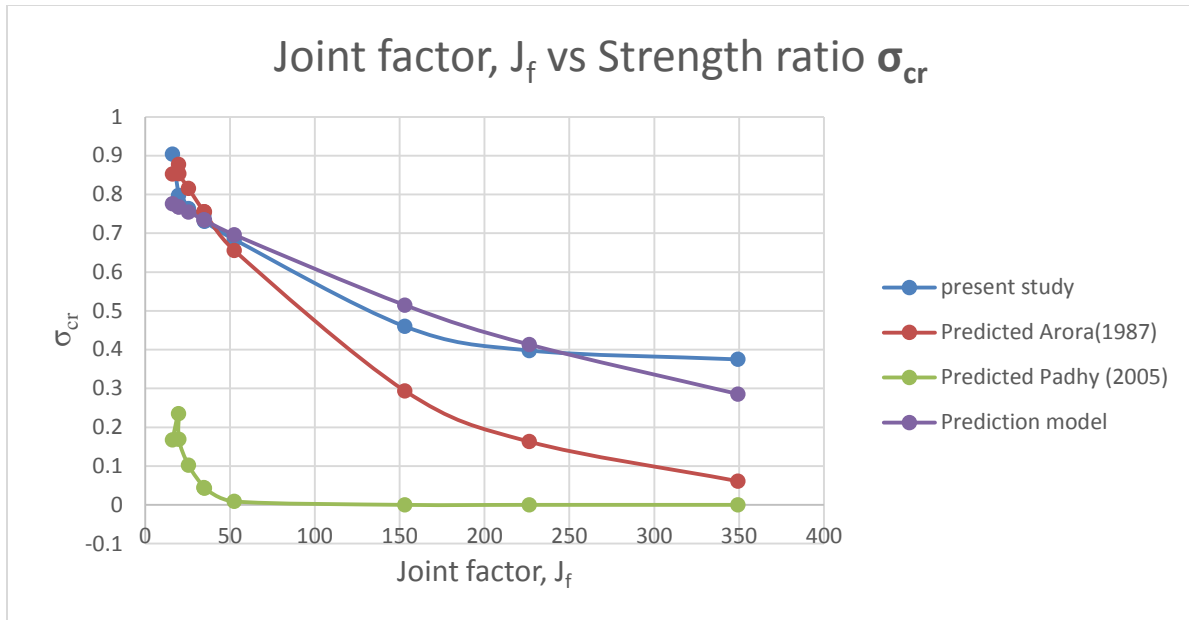


Figure 5.1: Comparison of uniaxial compressive strength ratio of prediction model with present study and empirical formulae (jointed specimen of plaster of paris, Single joint)

**Table 5.2:** Comparison of elastic modulus ratio of prediction model with present study and empirical formulae ( jointed specimen of plaster of paris, Single joint):

Joint factor, $J_f$	Present study $E_r = E_{tj} / E_{ti}$	Predicted Arora(1987) $E_r = e^{-0.0115 * J_f}$	Predicted Padhy (2005) $E_r = e^{-0.0125 * J_f}$	Prediction model $E_r = 0.892e^{-0.008 * J_f}$
19.839	0.797	0.796	0.780	0.761
34.933	0.785	0.668	0.646	0.674
153.040	0.3	0.172	0.148	0.262
349.331	0.05	0.018	0.013	0.055
226.327	0.2	0.074	0.059	0.146
52.514	0.538	0.545	0.519	0.586
34.557	0.614	0.672	0.649	0.676
25.346	0.629	0.747	0.727	0.728
19.741	0.712	0.797	0.781	0.762
16.069	0.85	0.831	0.818	0.784

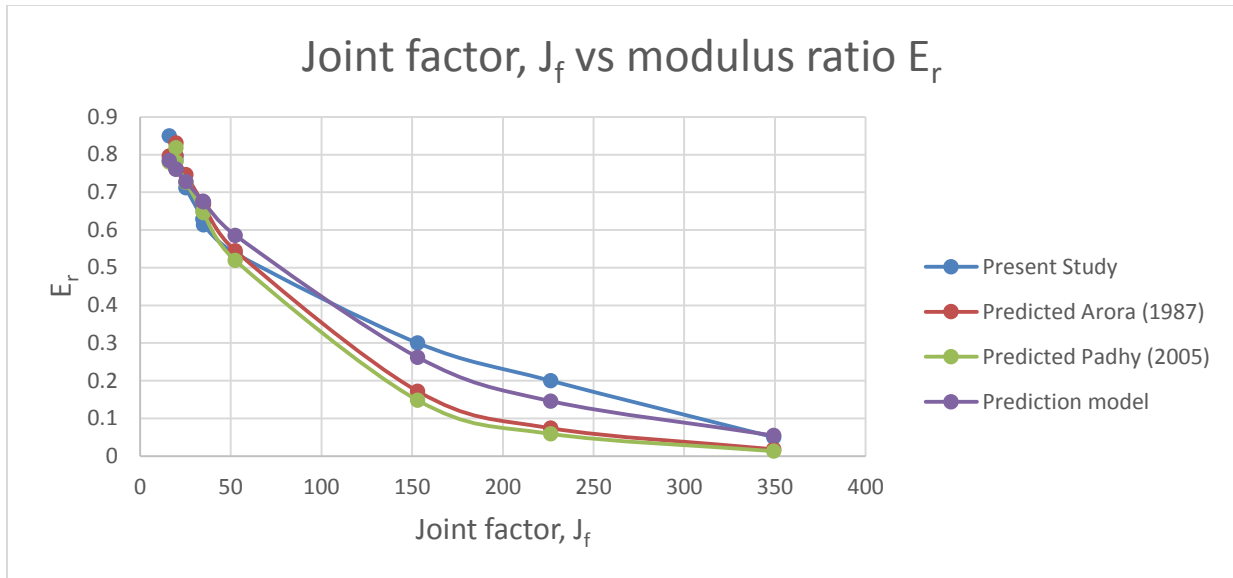


Figure 5.2: Comparison of elastic modulus ratio of prediction model with present study and empirical formulae ( jointed specimen of plaster of paris, Single joint)

**Table 5.3:** Comparison of uniaxial compressive strength ratio of prediction model with present study and empirical formulae (jointed specimen of plaster of paris, double joint):

Joint factor, $J_f$	Present study $\sigma_{cr} = \sigma_{cj} / \sigma_{ci}$	Predicted Arora(1987) $\sigma_{cr} = e^{-0.008 * J_f}$	Predicted Padhy (2005) $\sigma_{cr} = e^{-0.09 * J_f}$	Prediction model $\sigma_{cr} = 0.815e^{-0.003 * J_f}$
69.866	0.606	0.572	0.002	0.667
306.080	0.272	0.085	0.000	0.205
698.662	0.113	0.004	0.000	0.029
452.654	0.217	0.027	0.000	0.098
105.028	0.525	0.432	$8 * 10^{-05}$	0.559
69.115	0.609	0.574	0.002	0.669
50.692	0.724	0.667	0.010	0.736
39.482	0.746	0.728	0.029	0.776
32.138	0.820	0.772	0.055	0.805

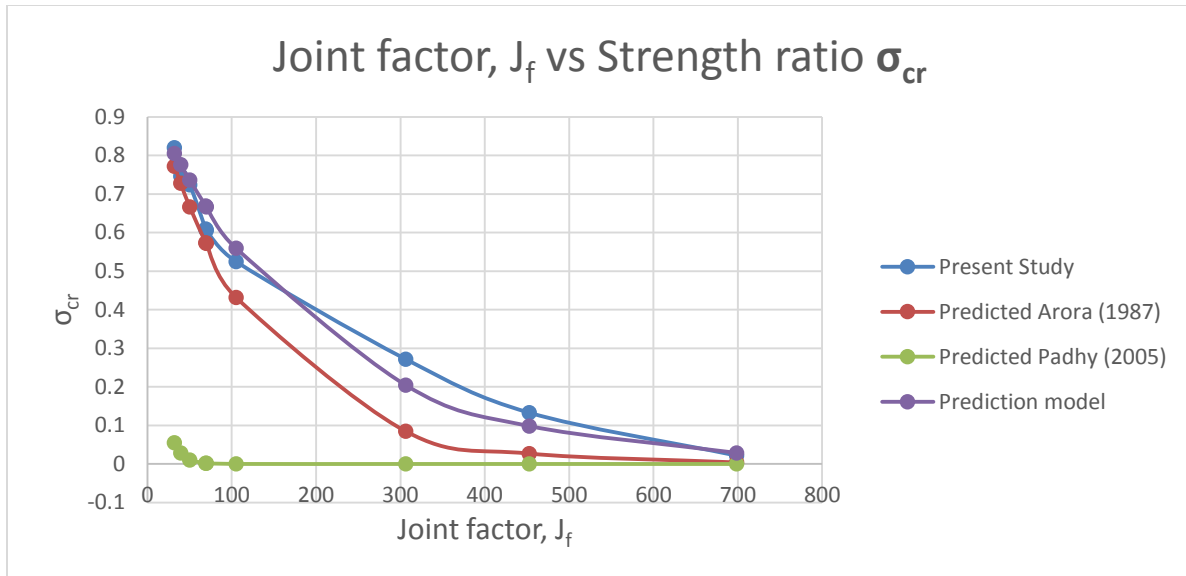


Figure 5.3: Comparison of uniaxial compressive strength ratio of prediction model with present study and empirical formulae (jointed specimen of plaster of paris, double joint)

Table 5.4: Comparison of elastic modulus ratio of prediction model with present study and empirical formulae ( jointed specimen of plaster of paris, double joint):

Joint factor, $J_f$	Present study $E_r = E_{tj}/E_{ti}$	Predicted Arora(1987) $E_r = e^{-1.15 \cdot 10^{-2} \cdot J_f}$	Predicted Padhy (2005) $E_r = e^{-1.25 \cdot 10^{-2} \cdot J_f}$	Prediction model $E_r = 0.892e^{-0.008 \cdot J_f}$
69.866	0.623	0.448	0.418	0.452
306.080	0.174	0.030	0.022	0.176
698.662	0.051	$3 \cdot 10^{-4}$	$2 \cdot 10^{-4}$	0.037
452.654	0.076	0.006	0.004	0.098
105.028	0.268	0.299	0.269	0.393
69.115	0.474	0.452	0.422	0.453
50.692	0.543	0.558	0.531	0.488
39.482	0.551	0.635	0.611	0.510
32.138	0.745	0.691	0.669	0.526

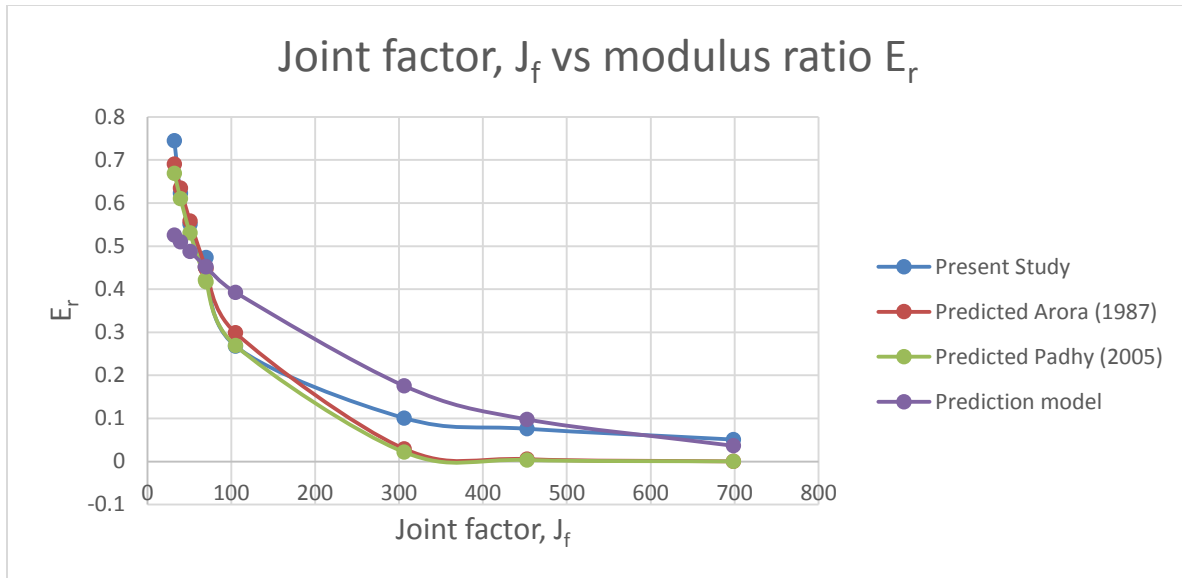


Figure 5.4: Comparison of elastic modulus ratio of prediction model with present study and empirical formulae (jointed specimen of plaster of paris, double joint)

**Table 5.5:** Comparison of uniaxial compressive strength ratio of prediction model with present study and empirical formulae (jointed specimen of plaster of paris-sand mix, single joint):

Joint factor, $J_f$	Present Study $\sigma_{cr} = \sigma_{cj} / \sigma_{ci}$	Predicted Arora(1987) $\sigma_{cr} = e^{-0.008 * J_f}$	Predicted Padhy (2005) $\sigma_{cr} = e^{-0.09 * J_f}$	Prediction model $\sigma_{cr} = 0.815e^{-0.003 * J_f}$
18.469	0.785	0.863	0.190	0.793
32.521	0.710	0.753	0.041	0.750
142.474	0.410	0.319	0.000	0.483
325.211	0.243	0.073	0.000	0.233
210.700	0.390	0.184	0.000	0.368
48.888	0.606	0.675	0.012	0.702
32.171	0.694	0.772	0.055	0.751
23.596	0.822	0.828	0.120	0.777
18.378	0.915	0.862	0.191	0.793
14.960	0.922	0.886	0.190	0.804



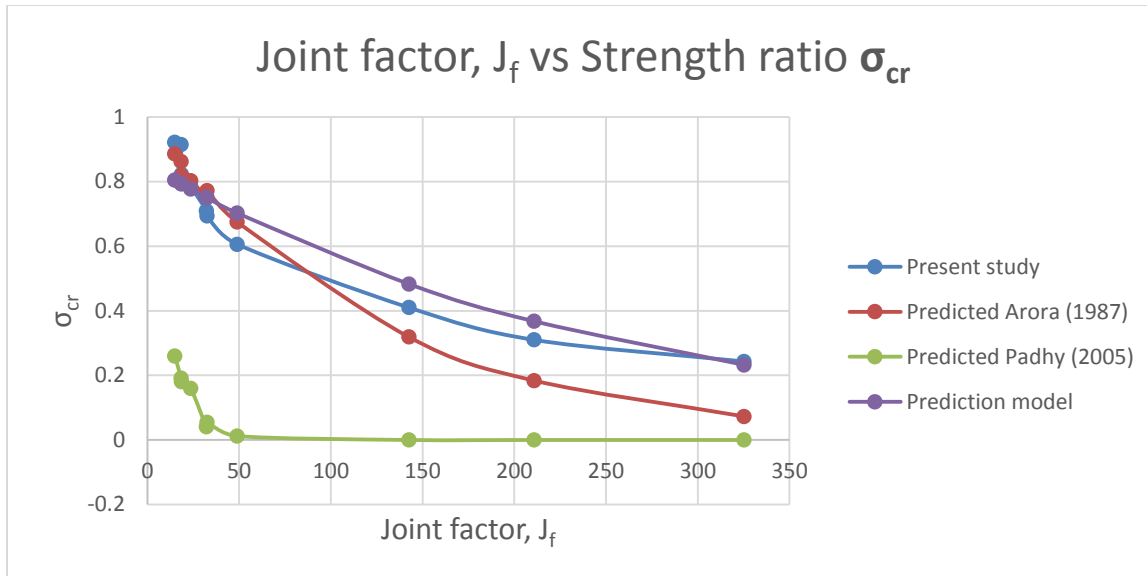


Figure 5.5: Comparison of uniaxial compressive strength ratio of prediction model with present study and empirical formulae (jointed specimen of plaster of paris-sand mix, single joint)

**Table 5.6:** Comparison of elastic modulus ratio of prediction model with present study and empirical formulae (jointed specimen of plaster of paris-sand mix, single joint):

Joint factor, $J_f$	Present study $E_r = E_{tj}/E_{ti}$	Predicted Arora(1987) $E_r = e^{-0.0115 * J_f}$	Predicted Padhy (2005) $E_r = e^{-0.0125 * J_f}$	Prediction model $E_r = 0.892e^{-0.008 * J_f}$
18.469	0.775	0.809	0.794	0.692
32.521	0.710	0.688	0.666	0.602
142.474	0.237	0.193	0.167	0.2
325.211	0.05	0.024	0.016	0.032
210.700	0.067	0.089	0.072	0.101
48.888	0.503	0.569	0.543	0.511
32.171	0.607	0.691	0.669	0.604
23.596	0.685	0.761	0.744	0.658
18.378	0.789	0.808	0.795	0.693
14.960	0.846	0.842	0.828	0.717

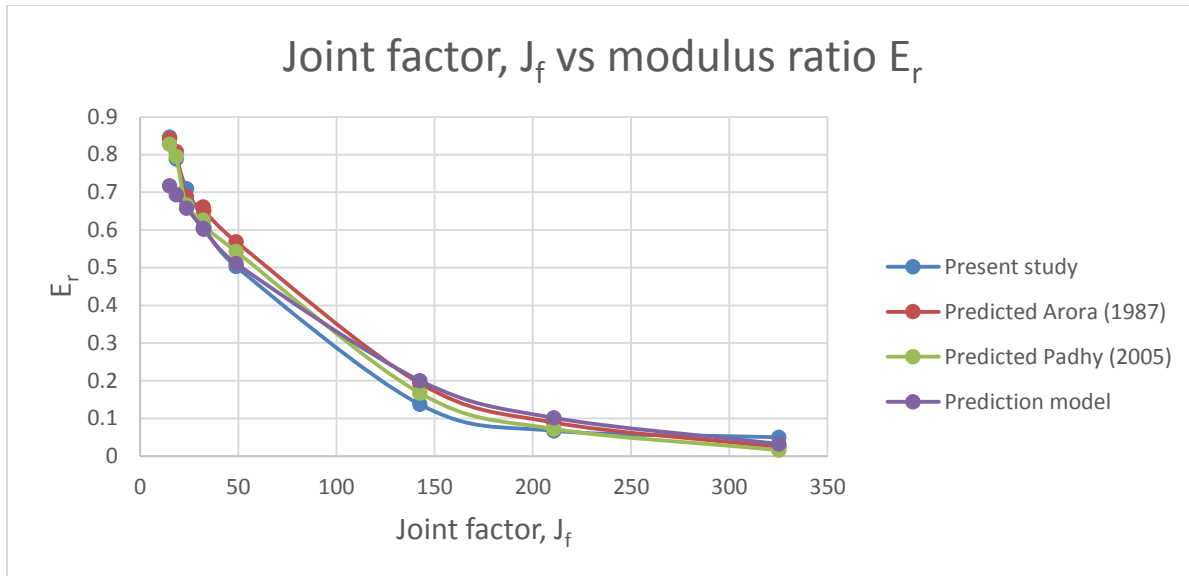


Figure 5.6: Comparison of elastic modulus ratio of prediction model with present study and empirical formulae (jointed specimen of plaster of paris-sand mix, single joint)

**Table 5.7:** Comparison of uniaxial compressive strength ratio of prediction model with present study and empirical formulae (jointed specimen of plaster of paris-sand mix, double joint):

Joint factor, $J_f$	Present Study $\sigma_{cr} = \sigma_{cj} / \sigma_{ci}$	Predicted Arora(1987) $\sigma_{cr} = e^{-0.008 * J_f}$	Predicted Padhy (2005) $\sigma_{cr} = e^{-0.09 * J_f}$	Prediction model $\sigma_{cr} = 0.815e^{-0.003 * J_f}$
65.042	0.608	0.593	0.003	0.59
284.947	0.243	0.101	0	0.305
650.423	0.192	0.005	0	0.102
421.401	0.253	0.033	0	0.203
97.776	0.498	0.456	$1 * 10^{-4}$	0.535
64.776	0.568	0.595	0.003	0.59
47.192	0.694	0.685	0.014	0.622
36.756	0.784	0.744	0.037	0.642
29.919	0.812	0.786	0.068	0.655

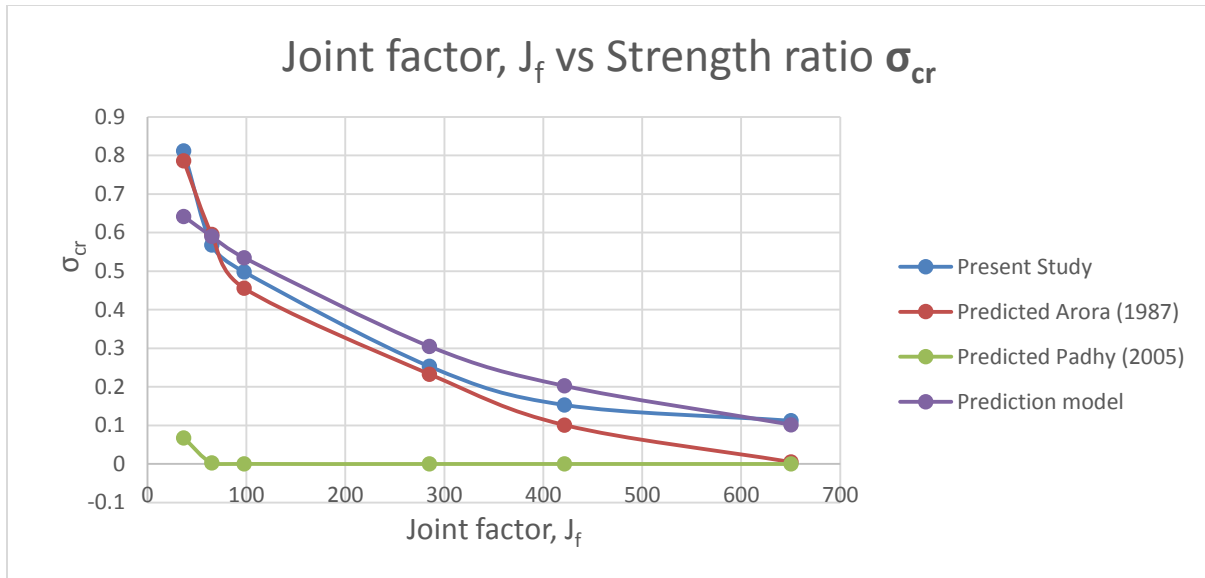


Figure 5.7: Comparison of uniaxial compressive strength ratio of prediction model with present study and empirical formulae (jointed specimen of plaster of paris-sand mix, double joint)

**Table 5.8:** Comparison of elastic modulus ratio of prediction model with present study and empirical formulae (jointed specimen of plaster of paris-sand mix, double joint):

Joint factor, $J_f$	Present Study $E_r = E_{tj}/E_{ti}$	Predicted Arora(1987) $E_r = e^{-0.0115 * J_f}$	Predicted Padhy (2005) $E_r = e^{-0.0125 * J_f}$	Prediction model $E_r = 0.892e^{-0.008 * J_f}$
65.042	0.623	0.473	0.444	0.461
284.947	0.132	0.038	0.028	0.191
650.423	0.060	0.001	0.000	0.044
421.401	0.123	0.008	0.005	0.111
97.776	0.387	0.325	0.295	0.405
64.776	0.476	0.477	0.447	0.46
47.192	0.554	0.581	0.554	0.5
36.756	0.690	0.655	0.632	0.52
29.919	0.737	0.709	0.688	0.531

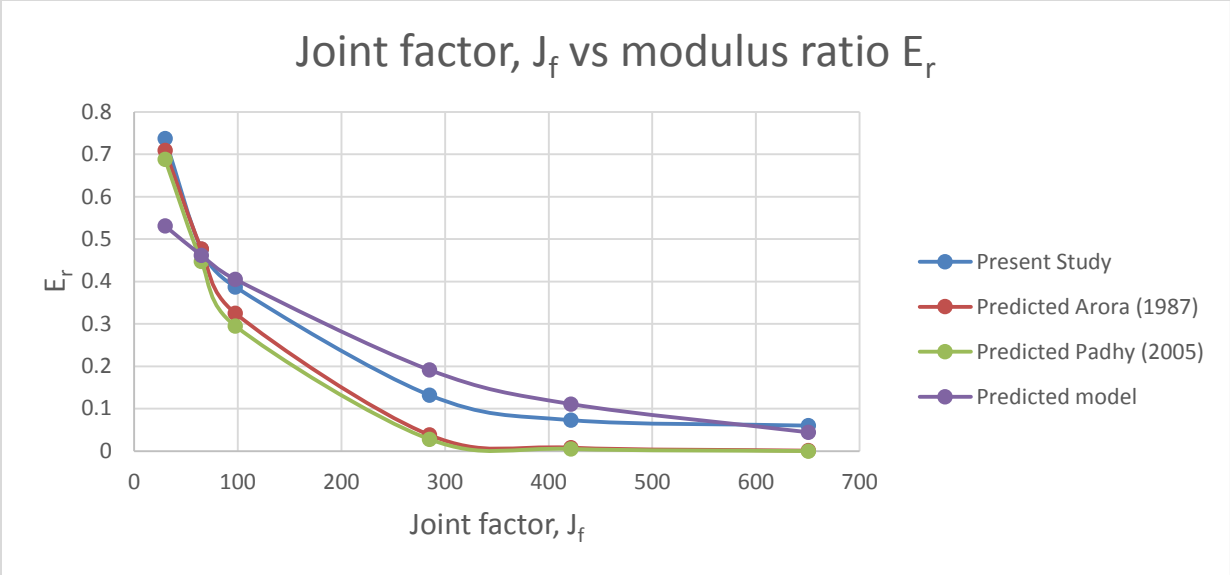


Figure 5.8: Comparison of elastic modulus ratio of prediction model with present study and empirical formulae (jointed specimen of plaster of paris-sand mix, double joint):

## Conclusion

On the basis of present experimental study on the intact and jointed specimen of plaster of Paris and plaster of paris- sand mix the following conclusions are drawn

- The strength of jointed specimen depends on the joint orientation  $\beta$  with respect to the direction of major principal stress. The strength at  $\beta=30^\circ$  is found to be minimum and the strength at  $\beta=90^\circ$  is found to be maximum.
- As the number of joints increases, the uniaxial compressive strength decreases.
- The values of Modulus ratio ( $E_r$ ) also depends on the joint orientation  $\beta$ . The modulus ratio is least at  $30^\circ$ .
- Average variation between proposed prediction model and present study found to be within 5%.
- Average variation between prediction model and predicted Arora (1987) found to be within 5%.
- Average variation between proposed prediction model and predicted Padhy (2005) for uniaxial compressive strength ratio found to be within 40% and for elastic modulus ratio average variation found to be within 5%
- Uniaxial compressive strength of Plaster of paris – Sand mix is found to more than uniaxial compressive strength of Plaster of paris for intact specimen as well as for jointed specimen.
- Also, elastic modulus ( $E_{ti}$ ) of Plaster of paris – sand mix is more than Elastic modulus ( $E_{ti}$ ) of plaster of paris for intact specimen as well as for jointed specimen

## **Scope of future work:**

1. Studies can be made on different model material to find the value of constant a and b in equation (iii) and (vi)
2. The effect of temperature, confining pressure and rate of loading on the strength characteristics can be studied.
2. Studies can be made by introducing multiple joints in varying orientation.
3. Strength and deformation behaviour of jointed specimens can be studied under triaxial conditions for the samples with number of joints.
4. Strength and deformation behaviour of jointed specimens under triaxial conditions can be studied with gouge-filled joints.
5. Prediction of strength and deformation behaviour of specimens with any arbitrary orientation and at any number of joints can be done by using artificial neural network with the help of these data's as well as data's from the literature also can be taken.
6. Numerical models can be developed by using different theories and the results can be compared with the experimental results to reach at the best possible Numerical Model.
7. Different software's can be used to analyses the experimental results.

## References:

1. Arora, V. K. (1987). "*Strength and deformation behaviour of jointed rocks.*" PhD thesis, IIT Delhi, India.
2. Arora, V.K. and Ramamurthy, T (1994) “ *Strength prediction for jointed rock in confined and unconfined states*” Int. J. Rock Mech. Sci. & Geomech. Vol.3 pp 9-22
3. Book: Engineering rock mass classifications by Z.T. Bieniawski
4. IS code: IS: 9143:1979 Method of determination of unconfined compressive strength of rock materials
5. IS code: IS 12634 : 1989 Rock joints-direct shear strength-Laboratory method of determination
6. IS code: IS 9179 -1979 Method for preparation of rock specimen for laboratory testing.
7. Jade, Sridevi and Sitharam, T.G. (2003) “*Characterization of strength and deformation of jointed rock mass based on statistical analysis*” ASCE (2003) International journal of geomechanics vol.3 10. 1061/(ASCE)1532-3641 (2003)3: 1(43)
8. Lama, R. D. (1974). "Uniaxial compressive strength of jointed rock." *Institute of soil mechanics and rock mechanics*, P-Muller Festschrift.ed., Karlsruhe,Germany, 67- 77.
9. Singh, M and Rao, K.S. and Ramamurthy, T. (2003) “*Strength and Deformational Behaviour of a Jointed Rock Mass*”, SPRINGER Rock Mech. Rock Engng. (2002) 35 (1), 45–64
10. Thaweeboon, Saisuree and Dasri, Ronnachai (2016) “ *Strength and deformability of small scale rock mass models under large confinement*”, SPRINGER(2016) Bull Eng Geol Environ 10.1007/s10064-016-0871-9
11. Tiwari, R.P and Rao, K.S (2006) “*Deformability characteristics of a rock mass under true-triaxial stress compression*” SPRINGER (2006) Geotechnical and Geological Engineering (2006) 24: 1039–1063.
12. Xin, Chen and Zhihong, Liao (2012) “*Deformability characteristics of jointed rock masses under uniaxial compression*” ELSEVIER International Journal of Mining Science and Technology 22 (2012) 213–221
13. Yaji, R. K. (1984). "*Shear strength and deformation of jointed rocks*" PhD thesis, Indian Institute of Technology, Delhi, India.